10th semester

CHEMICAL RECYCLING AND REPURPOSING STRATEGIES FOR EPOXY-BASED THERMOSETS: TOWARD FUNCTIONAL CIRCULARITY

June 2025

Materials Technology, Virginia Rosa-Maria Margherita Cremonese
Department of Materials and Production, Aalborg University

AALBORG UNIVERSITY
STUDENT REPORT

Aalborg University
Department of Materials and Production
Study Board of Physics and Mechanics
www.mp.aau.dk

Title:
Chemical Recycling and Repurposing Strategies for Epoxy-Based Thermosets: Toward Functional Circularity

Semester:
10th semester

Project period:
February 2025– June 2025

Email:
vcremo22@student.aau.dk

Supervisors:
Prof. Lars Rosgaard Jensen

Number of pages:
42

Number of appendix pages:
53

Finish date:
June

Abstract:

The growing need for sustainable material management in polymer science has intensified research into the recyclability of thermosetting polymers, particularly epoxy resins, which are notoriously difficult to process due to their irreversible crosslinked structures. This study addresses the challenge of chemically recycling an epoxy-based thermoset through a controlled dissolution methodology aimed at depolymerizing the cured network into a reusable form. The work involves a systematic investigation of the transformation process—from the initial breakdown of the cured resin into a powder form, to its subsequent dissolution and analysis—focusing on the rationale behind both successful and failed technical approaches.

In parallel, the study explores alternative value-added applications for the recyclate, transitioning from a thermoplastic processing route to its reformulation into a new resin system, and ultimately its use as an adhesive material. These investigations aim to reposition the recyclate not merely as waste but as a functional material with viable industrial applications, thereby contributing to circular economy strategies in polymer design.

Preface

The following Master's thesis was written by Virginia Rosa-Maria Margherita, 4th semester Materials Technology at Aalborg University, under the supervision of Professor Lars Rosgaard Jensen. The project period was from the 1st of February 2025 to the 13th of June 2025.

In this project the structure-property relations of recycled epoxy laminate was analysed both chemically and mechanically wise. The scope of this project was to find a possible repurpose for the polymeric matrix of composites, after the recycling process, in order to have a closure of the loop for epoxy-based thermosets, aligning with circular economy principles.

Tables, figures, and equations are numbered in order of appearance. Citations are listed in alphabetical order with [citation number]. Full references are shown in the bibliography.

Acknowledgements are given to my supervisor for his help and guidance in theories and experimental work, and for his great support. Furthermore, the laboratory team at Fibigerstræde 14 has been fundamental in assistance with testing setup. Special thanks to my family and my friends for their constant support and cheering up in the most difficult moments.

June 2025.

Virginia Rosa-Maria Margherita Cremonese

Contents

1 Introduction

Polymers, commonly called plastics, are deeply integrated into our society, due to their incredible versatility, low price, durability, corrosion resistance, and excellent thermal and electrical insulation properties [1]. According to Conversio Market & Strategy GmbH and nova-Institute, about 400.3 million metric tons (Mt) of plastics were globally produced in 2022 [2]. Recent estimates report that between 1950-2015 approximately 8300 Mt of virgin plastics were produced. In 2015, the plastic waste generated amount of 6300 Mt, of which only 9% have been recycled, 12% was incinerated, and 79% was accumulated in landfills or the natural environment [3] The effects of such a huge quantity of plastic waste on the natural environment and human living environment are disturbing [4]. Hence, the urgency to improve the recyclability of plastic materials.

Of the most widely used plastics today, thermoset polymers, due to their great solvent resistance, excellent mechanical and thermal properties, are of great interest. Indeed, they account for about 14.1% of the global plastic production volume [2]. The presence of covalent intramolecular crosslinks, gives thermoset polymers their performing properties. Nonetheless, due to their chemical structure thermosets cannot be reshaped or recycled, either with melting or solution processing, hence representing a major problem in their disposal [5].

Among thermosets, epoxy resins are widely used across a wide range of fields such as high-performance coatings, electronic materials, general-purpose adhesives, and matrices for high-performance composites because of their outstanding mechanical properties, corrosion resistance, high adhesion strength, chemical resistance, good heat resistance, and high electrical resistance [4, 6, 7]. A very important application of epoxy resins is placed in wind energy [8]. This sector is growing fast, both in terms of number of turbines and in their sizes. Modern turbines are 100 times bigger than those in 1980 [9]. While this increasing demand for clean energy is positive for more sustainable energy production, the decommission of the wind turbine remained an issue. Among the different components, the blades represent the greatest problem, due to the precence of very high proportion of fibre-reinforced polymers (FRPs), such as glass fibre-reinforced polymer (GFRP) or carbon fibre-reinforced polymer (CFRP) [10–12]. The lifecycle of wind turbine blades is known to be approximately 20-25 years, after which they face decommissioning challenges due to the difficulty in recycling their composite materials. Indeed, it is estimated that there will be about 43 million tonnes of blade waste worldwide by 2050, China contributes 40%, Europe 25%, the United States 16%, and the remaining 19% comes from the rest of the world [13].

A number of different recycling strategies have been developed for epoxy thermosets and its composites. There are substantially two different categories to address the recovery: those that, by mechanical commutation techniques, introduce dynamic reversible bonds to produce new types of recyclates; and those that recover the scrap into chemical, materials and energy [4, 8, 14–16]. In particular, for epoxy thermosets, a great focus is on physcycling and chemcycling [4]. Physcycling refers to the mechanical recycling of epoxy thermosets, where the materials are broken down

into smaller pieces and reused without changing their chemical composition. Chemcycling, on the other hand, involves chemically breaking down the epoxy thermosets to recover valuable chemicals and components, which can then be used to synthesize new materials. When subjected to non-selective chemcycling, the chemical structure of the epoxy matrix is largely destroyed because the cleavage of bonds is not on specific groups, which makes the recovery difficult. Moreover, it not only degrades the use of polymer matrices, but also compromises the properties of reinforcing fillers, such as fibres. In this regard, the selective degradation of the bonds is of crucial importance. For amine-cured epoxy, the selectivity of bond breaking of C-N bonds results in being quite difficult due to the difference in activation energy between the C-N bonds and the ester bonds [17]. Therefore, to preserve the valuable carbon skeleton to obtain high-value products a selective cleavage of chemical bonds is essential [4].

Researchers have developed methods to recycle cured epoxy resin by breaking it down using acid solutions, as technically detailed in Section 2.3. However, until now, recycling of cured epoxy resin to reuse in new products are not success: e.g., Dubey et al. report how they have only been able to recycle the recovered thermoplastic by compounding with an 80% wt of polyethylene [18].

To find an effective epoxy-based thermoset polymer recycling and repurpose, this work focuses on the dissolution-based depolymerization of a cured epoxy resin, followed by characterization of the resulting recyclate. The thesis further investigates alternative valorization strategies for the recyclate, including thermoplastic processing, resin reformulation, and adhesive applications, aiming to expand the functional reuse of epoxy-based materials within a circular economy context.

The methodology adopted in this thesis to address this problem evolves towards two primary directions: one dealing with the material and the procedural processes and the other one on the application approaches.

The first direction is related to the material's representation and processing methodology, detailing the dissolution (recycling) of the epoxy-based materials, and subsequent neutralization and transformation into a powder form, followed by its dissolution. Technical choices are discussed and motivated, addressing both successful and unsuccessful approaches, and elucidating the rationale behind the latter's negative outcomes. The final experimental procedure and subsequent analyses are described in Chapter 4, where a thorough examination of the FTIR spectra is used to support the hypothesis. A series of separate material batches were fabricated and analysed, with initial experimentation carried out to investigate the material's functionality and behaviour. A comprehensive explanation for the successful and unsuccessful results is given, citing various mechanistic and physicochemical factors that may have or may not have contributed to this outcome and why. These factors collectively suggest that the re-crosslinking process did not occur due to a combination of these elements.

In the second direction, different possible applications of recyclate are studied: the implementation of an initial thermoplastic material processing strategy, then the transition to a novel resin-based approach, and the adoption of the material as an adhesive in the final stage.

In summary, this thesis addresses one of the major challenges in polymer sustainability by exploring the chemical recycling and functional repurposing of epoxy-based thermoset resins, materials traditionally deemed non-recyclable. The main achievements are as follows:

- This work demonstrates the potential to reuse and valorise epoxy recyclate across diverse applications from thermoplastic blending to adhesive reengineering by using Recyclamine®-enabled formulations and a dissolution-based depolymerization process.
- By integrating analysis at molecular level with application testing, the study provides both scientific insight and practical direction toward embedding epoxy thermosets within a circular materials economy.

The outcomes are intended to inform not only recycling strategy development but also material design choices for future generations of sustainable polymers.

The complete structure of this report after this introduction is as follows: In Chapter 2, the chemistry of the epoxy resin and different approaches for their recycling are presented, with details on the process of epoxy monomers formation, on the classification of the epoxy resin, and on the chemistry of curing process. In Chapter 3, the materials used are presented, together with the methods for the pre-sample preparation - using a laminate manufacturing, a laminate recycling, a precipitation method and an up-concentration process - as well as the analytical techniques used to analyse the materials, namely: FTIR, TGA, DSC, Injection moulding, Tensile testing and the characterization of adhesion ability. Chapter 4 introduces the curing reaction between the epoxy resin and the hardener, and thoroughly discusses the analytical results obtained. Several interesting results are presented, highlighting, however, that the powder production process has demonstrated inconsistency, and providing some educated guesses for that. Moreover, an overview on possible way to up-concetrate the recyclate in solution form is presented. In Chapter 5, the applications of recyclate that have been tested are discussed and analysed: the recycled polymer powder was tested as thermoplastic polymer, to use it together with the virgin epoxy resin in the composites production, and as a structural adhesive. The Conclusion and Outlook chapter, Chapter 6, summarises the work and provides some potential directions for future work. The Appendix A (7) reports the additional attempts and analysis that were performed.

Theory 2

2.1 Chemistry of Epoxy Resin

The overarching problem addressed in this thesis is the development of an effective strategy for the recycling and functional reuse of epoxy-based thermosets. This chapter provides a detailed overview of the chemical structure and synthesis of epoxy resins, and explores the various classifications of epoxy systems based on their functionality and application. Particular emphasis is placed on the curing process—typically involving polyamine or anhydride hardeners—which leads to the formation of a rigid, three-dimensional thermoset network through irreversible covalent crosslinking.

In light of the urgent need to improve the sustainability of recycling epoxy-based materials, this chapter also surveys the state-of-the-art in recycling strategies, including mechanical, thermal, and chemical approaches. Special focus is given to chemical recycling methods aimed at depolymerizing the crosslinked network, thereby recovering value-added products or enabling repurposing of the material.

2.1.1 Formation of Epoxy Monomers

The term *epoxy* refers to a class of polymeric material characterised by the presence of one specific 1,2-epoxide which is a three-membered oxirane ring (Figure 2.1), generally called epoxide. Whereas, by definition, *epoxy resin* defines the range of uncrosslinked bi- or multifunctional epoxides, i.e. molecules containing two or more epoxy groups [19–21]. However, the term *epoxy resin* is commonly used to refer to cured epoxy resins even if they contain very little or no epoxy groups.

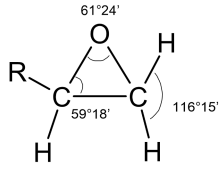

Figure 2.1: Three-membered oxirane ring characteristic of epoxy resins.

Epoxides can be prepared by using different methods. The most common way of making epoxides is the electrophilic reactions of alkenes with peroxy acids (also referred as peroxycarboxylic acid), such as peroxyacetic acid. The mechanism, reported in Figure 2.2, involves the nucleophilic π bond electrons of the alkene attacking the peroxy acid oxygen, breaking the $O-O$ bond bringing to the formation of a new carbonyl, and the starting bounding to the hydroxyl's hydrogen. The electrons from the hydroxyls still free are then involved in the formation of a covalent bond between the electrophilic carbon from the π bond.

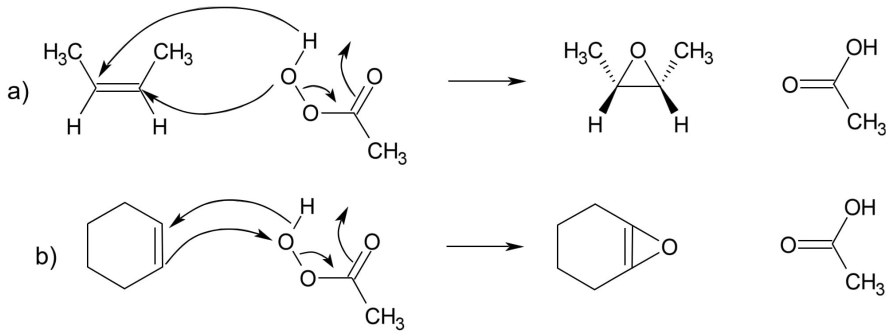

Figure 2.2: Reaction mechanism for epoxidation of the alkene of a) but-2-ene and b) cyclohexene.

Another approach for preparing epoxides is the intramolecular S_N2 reaction of halo alcohols (halohydrins) by treatment with a strong base (Figure 2.3).

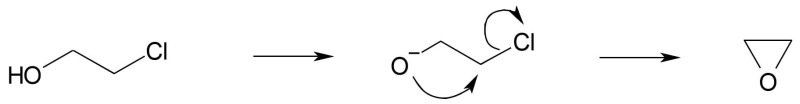

Figure 2.3: Reaction mechanism for epoxidation of 2-Chloroethanol.

The high chemistry versatility of the three-membered oxirane ring is is partly attributed to its bond strain, which makes it prone to both nucleophilic and electrophilic ring-opening reactions [20, 22]. This ring stain arises due to the deviation from the ideal tetrahedral $O-C-O$ or bond angle of 109.5°. Since the oxirane ring angle is about 61°, the interaction between adjacent bonds occurs via orbital overlap., hence the normal sp^3 hybridization of the linear bond with the ring atoms, is impossible. Together, these factors make the epoxides highly reactive, as relieving this strain is energetically favourable. The most important reaction for oxirane groups in the synthesis of curing of epoxy resins proceed either by nucleophilic attack of the carbon atoms from the epoxide ring or by electrophilic attack on the oxygen atom.

In nucleophilic ring-opening reactions, a nucleophile attacks the electrophilic carbon atoms of the unsymmetric epoxide ring. Under basic or neutral conditions, this attack predominantry occurs at the least hindered site, proceeding via an S_N2 mechanism. This pathway leads to the inversion of configuration at the site of attack, where $Nu-C$ bond is forming and the $C-O$ bond is breaking (Figure 2.4 a). Differently, under acid conditions, the epoxide oxygen is protonated, and a partial positive charge is formed on the more substituted ring carbon, enhancing its electrophilicity. The nucleophilic attack hence occurs at the more substituted carbon (Figure 2.4 b). This behaviour exhibits both S_N1 and S_N2 mechanism characteristics. While a "full" carbocation is not formed, the partial positive charge on the more substituted carbon in the ring of the transition increases the reactivity, favouring a nucleophilic attack at the more substituted carbon. However, even though the reaction shows regioselectivity S_N1 character, the intermediate state formation retains partial S_N2 character, since steric hindrance affects the ability of the nucleophile to approach the electrophilic carbon. Hence, the reaction appear to present a "borderline" S_N2 mechanism [23, 24].

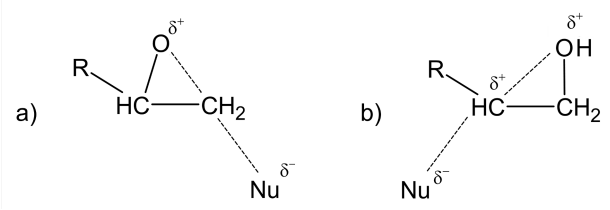

Figure 2.4: Nucleophilic addiction mechanism to the oxirane ring: a) under basic and neutral conditions (S_N2 mechanism) a) under acidic conditions ("borderline" S_N2 mechanism). Adapteb from [25].

2.1.2 Classification of Epoxy Resin

The monomer used in the production of epoxy resins can be divided in two families: the glycidyl epoxies and non-glycidyl epoxies [26]. Non-glycidyl epoxies, along with monofunctional epoxies, are mostly used as reactive diluents, viscosity modifiers, and adhesion promoters. Non-glycidyl epoxies can be either aliphatic or cyclo-alyphatic, and are produced by the peroxidation of olefinic double bonds. Glycidiyl epoxy are synthesized through a condensation reaction involving epichlorohydrin and compounds such as dihydroxy compounds (e.g. bisphenol-A), dibasic acids, or diamines [6, 27–29].

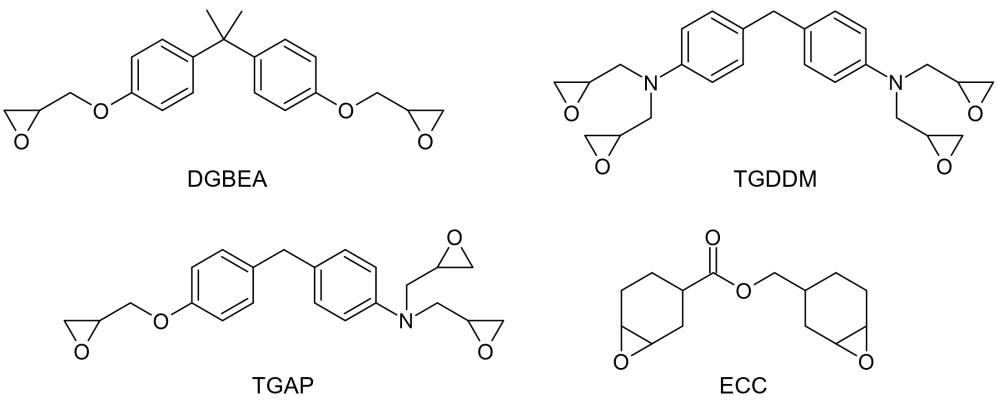

Figure 2.5: Structure of the most common employed epoxy monomers.

Diglycidyl ether of bisphenol A (DGEBA), obtained by by reacting bisphenol A with an excess of epichlorohydrin in the presence of sodium hydroxide catalyst, is by far the most used epoxy resin monomer, as it is used in 75-90% of epoxy resin systems [30]. Multifunctional epoxy monomers are pivotal for advancing the performance as well as the applicability of epoxy resins across various different industries. These monomers are characterised by multiple reactive sites, which enable densely cross-linked networks to form. This results in materials displaying improved mechanical strength, thermal stability, and chemical resistance [31]. For instance, epoxy resin monomers derived from multifunctional aromatic glycidyl amine resins, such as N,N,O-triglycidyl-p-aminophenol (TGAP) and N,N,N',N'-tetraglycidyl-4,4'-diaminodiphenylmethane (TGDDM), present high glass transition temperatures, which contribute to superior thermal stability and mechanical performance at elevated temperatures, making them suited for advanced applications [32, 33]. Another class of great interest are cycloaliphatc epoxy resins. Because of their nature, they present high UV resistance and a lower level of yellowing compared to aromatic epoxy resins [34]. An examples of this category is 3,4-epoxy cyclohexylmethyl 3,4-epoxy cyclohexane carboxylate (ECC) [34]. The chemical structures of the most commonly used epoxy monomers are reported in Figure 2.9.

2.1.3 Chemistry of Curing Process

In order to transform liquid epoxy resin into a hard, infusible thermoset network the addition of curing agents, also known as hardeners, is essential. These components promote the cross-linking, or curing, of epoxy resins [35]. Depending on the type of curing agent, curing mechanism can proceed though either chain-growth ring-opening polymerization or step-growth polymerization [21]. Chain-growth process can occur by anionic ring-opening homopolymerization or by cationic ring-opening homopolymerization initiated by catalytic curing agents [25, 36]. Whereas, when the curing process occur by polyaddition or copolymerization reaction with a multifunctional curing agent, it follows a step-growth mechanism [20].

Cationic ring-opening polymerization of epoxy monomers is generally initiated by Lewis acid such as boron trifluoride complexes [37] and onium salts including diaryl iodonium, triarylsulfonium or phosphonium salts and strong Brønsted acid HMtFn - where Mt is a metalloid (such as B, P, As or Sb) and n is the number of fluorine atom bound to the metalloid centre (for B n=4, whereas for P, As and Sb n=6) - such as fluoroboric acid [38–40]. In most applications, strong Brønsted acid $HMtF_n$ are actually initiating the cationic polymerization. Indeed, when an onium salt undergo photolysis or thermolysis and also when a BF_3-amine complex go through thermolysis or hydrolysis, Brønsted acid is released [36] (Figure 2.6 a). Epoxy monomers are then rapidly activated (Figure 2.6 b). Propagation proceeds through the ring-opening polymerization mechanism, where an oxonium active centre at the end of the growing chain very quickly react with new monomers (Figure 2.6 c). One of the most common termination steps for the cationic homopolymerization is involve the combination of the propagating oxonium ion and an anion derived from the counteranion. In the case of BF_4^-, the propagating oxonium cation can be attaked by the weakly nucleophilic F^- ion, as shown in Figure 2.6 d.

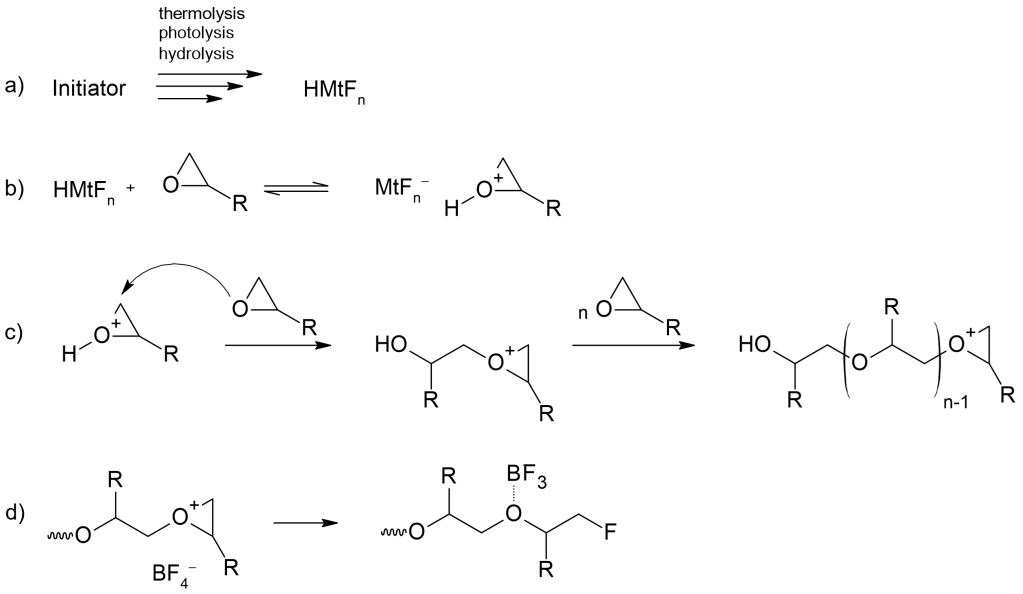

Figure 2.6: Reaction mechanism of cationic ring-opening polymerization: a) formation of a strong Brønsted acid $HMtF_n$ where Mt is classically B (n=4), P (n=6), As (n=6) or Sb (n=6), b) initiation by a strong Brønsted acid, c) propagation through an oxonium active centre at the end of the growing chain d) possible termination by the combination of the propagating oxonium with the anion derived from the counteranion (i.e. F^- in this example).

Anionic ring-opening polymerization is typically initiated by tertiary amines, in particular, imidazoles are recognised to be highly effective and fast-acting curing agents. Nonetheless,

imidazoles require to be stabilized, as their instability is not suited for one-pot epoxy formulations, making them impractical for products that need a long shelf-life before curing [41]. For this reason, the initiators are designed to release tertiary amines only when subjected to heat or light stimuli (Figure 2.7 a). The polymerization mechanism is based on the formation of alkoxide (Figure 2.7 b), which reacting with the epoxy monomer to generate a new alkoxide and continue the polymerization chain [21] as displayed in Figure 2.7 c. The termination step can occur through N-dealkylation or the β-elimination of the N substituent from the growing chain [42]. Epoxies can also undergo copolymerization with other cyclic monomers through anionic chain polymerization. Notably, epoxy-anhydride formulations cured with tertiary amine initiators have been described as an alternating epoxy-anhydride anionic copolymerization [43, 44], even though the mechanism is way more complex due to the polyetherification of excess epoxy groups [45] and the possible formation of carboxylic acid by esterification of hydroxyl groups with the anhydride and the following epoxy-acid esterification [46, 47]. Recently, several authors reported the possibility of using commercial ionic liquids, such as dialkylimidazolium ions, as latent initiators [36].

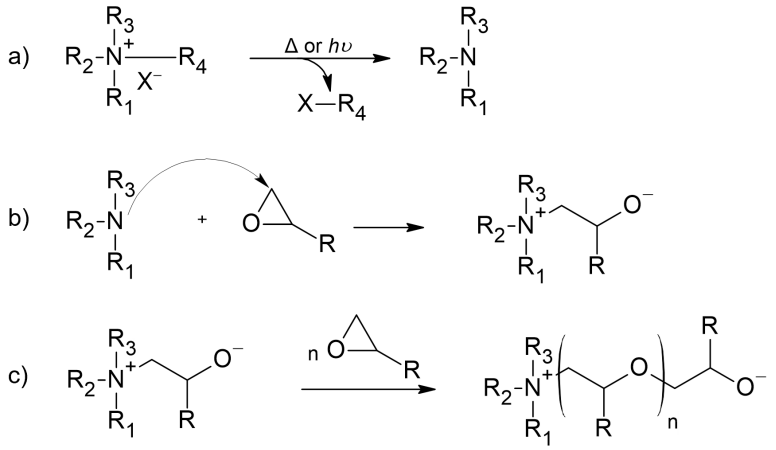

Figure 2.7: Reaction mechanism of anionic ring-opening polymerization: a) decomposition of the stabilized imidazole in tertiary amine, b) initiation by tertiary amine, c) propagation through the formation of an alkoxide, which attacks an epoxy monomer producing a new alkoxide and so on.

Epoxy resins can be cured using a variety of coreactants, such as amines, acids, isocyanates, and mercaptans, through step-growth polymerization processes [24]. Of these coreactants, polyamines are the most typically used [48, 49]. In this case, both the hydrogen atoms of the amino group parecipate successively in the ring-opening addiction reaction between the oxirane ring and the amino group (Figure 2.8 a). The reactivity of the system and, thereby, the kinetics of the curing process, is defined by the nucleophilicity of the amine and the electrophilicity of the epoxy group. It my be remarked that the kinetics are not equal because of the difference in induction and steric effect of the hydrogen atom of the primary and secondary amine. Indeed, secondary amino groups are less reactive than primary amino groups. As mentioned in Section 2.1.2, epoxy resin are commonly a derivative of DGEBA, so that the nucleophilicity of the amine is the main factor affecting the reactivity of the system. Additionally, the reaction is catalysed by the formation of hydroxyl groups induced by the ring-opening reaction of epoxy groups. In the absence of catalysts its proceeding is autocatalytic [48]. Here, as displayed in Figure 2.8 c, the hydroxyl groups participate in hydrogen bonding, forming reversible trimolecular complex that promotes the nucleophilic attack of the amino group.

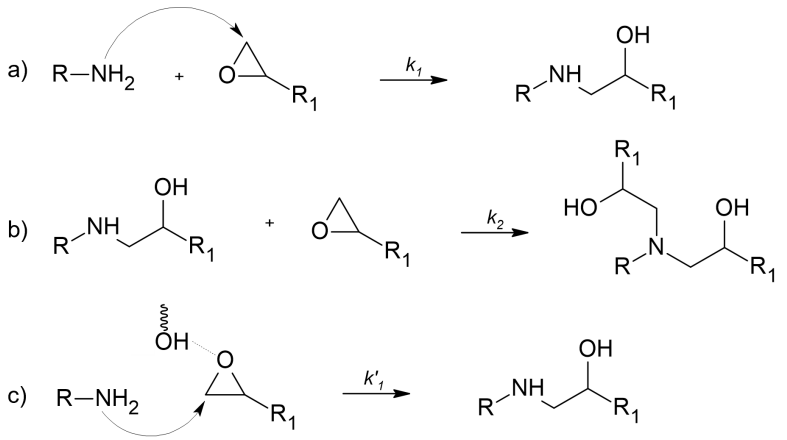

Figure 2.8: Reaction mechanism of step-growth ring-opening polymerization: without autocatalytic reaction a) firstly a primary amino group reacts with the oxirane ring forming a secondary amine that b) react with a new epoxy group; c) with an autocatalytic reaction a trimolecular complex is formed promoting the the nucleophilic attack of an amino group to an epoxy group.

In epoxy resin systems a relevant characteristic is the pot-life, i.e. the time interval following the mixing of the epoxy resin with the curing agent during which the mixture remains in a workable, low-viscosity state suitable for processing and application. Specifically, thermal latent curing agents, which are activated by external stimulation and guarantee stability, primarily function through two distinct mechanisms. The first involves the insolubility of the hardener in the epoxy resin due to its crystalline character, which becomes soluble and active after passing its melting point. The second mechanism relies on a precursor compound, which remains inactive at room temperature but activates when triggered by a rise in temperature [50]. The pot-life of a two-component epoxy system is primarily determined by the reactivity of the curing agent with the epoxy groups. A commonly employed strategy to control step-growth ring-opening polymerization involves modulating the nucleophilicity of the hardener. For example, diaminodiphenylsulfone (DDS) may have pot-life of multiple months, while for diethylenetriamine (DETA), typically has a pot-life of no more than twenty minutes [36]. This is because aromatic amines are weaker nucleophiles than aliphatic ones, hence less reactive. Another common approach to reduce reactivity is the use of high melting point, insoluble curing agents [21]. One of the most widely used latent curing agents is dicyandiamide (DICY) [24, 51]. The latent character of this solid arises from its insolubility in epoxy resins at room temperature, which guarantees the system a pot-life of up to one year [36]. Upon heating, either with or without catalysts, rapid polymerization is initiated. However, elevated temperatures are required to trigger the reaction. For this reason, DICY is typically used in combination with co-curing accelerators or catalysts, as the uncatalyzed reaction with epoxy resins does not begin until temperatures exceed the melting point of DICY (150°C) [52]. Moreover, residual crystalline cluster in the cured matrix can act as structural crosslinking domains influencing the mechanical properties [53]. Furthermore, dihydrazides are other amine used as latent curing agents. Similar to DICY, they present a high crystalline character, hence they can be easily dispersed in liquid epoxy resins. A strong correlation between the melting point of the dihydrazide and the initial curing temperature of the system was observed by Tomuta et al. [50]. Moreover, unlike other aliphatic amines, which commonly react with epoxy resins at room temperature, aliphatic dihydrazide where shown to exhibit very high curing temperatures. This behaviour can be explained by the moderate nucleophilic character of the NH_2 groups of the dihydrazides, as their election density is considerably diminished by the adjacent NH group.

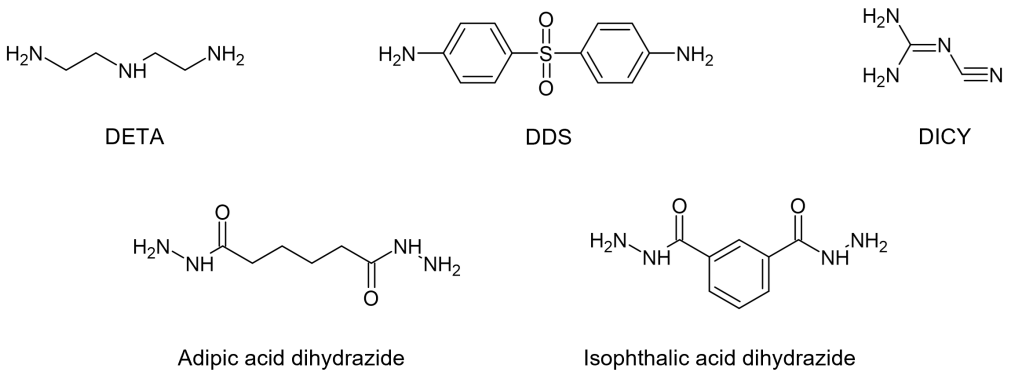

Figure 2.9: Structures of common amine hardeners for epoxy resins.

The production of single-phase systems with long shelf-life, has been reported to be possible through various strategies involving the protection and deprotection of the amino group of the curing agents [54, 55]. One widely studied approach involves ketone-based imines, which serve as moisture-activated latent hardeners. The very low nucleophilicity of the ketimines, due to the steric hindrance repulsion between the epoxy and the nitrogen atom, especially with bulkier ketones, results in extended shelf-life of the mixture. Upon atmospheric moisture exposure (i.e. an aqueous acetic environment), imine hydrolysis regenerates the amine (Figure 2.10 a), initiating curing [24]. Though stable, ketimines are not completely unreactive with epoxies due to the possible formation of a nucleophilic sited by enamine-imine tautomerism (Figure 2.10 b). However, the evaporation of ketones raises concerns due to the emission of volatile organic compounds (VOCs).

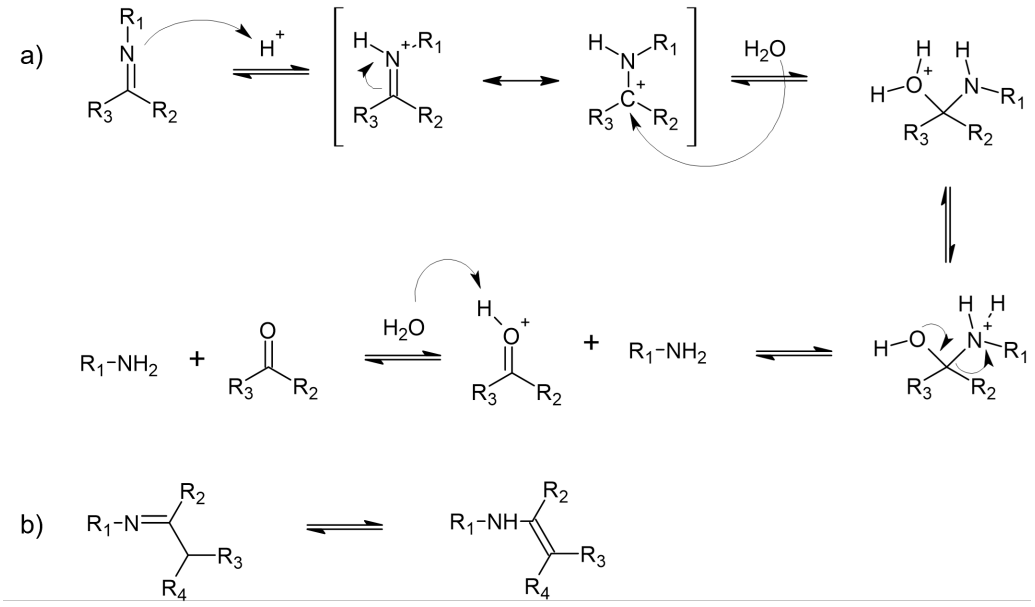

Figure 2.10: a) Regeneration of an amine by imine hydrolysis after exposure to atmospheric humidity. The reaction starts by protonation of the imine nitrogen. The resonance-stabilized cation that forms, which is very electrophilic, is then attacked by a molecule of water. A primary amine is released after a proton transfer from the oxygen to the nitrogen. This step generates an oxonium ion which deprotonating forms a ketone. b) Tautomeric equilibrium between the imine and the enamine.

2.2 Recycling Methods for Epoxy Resins

The inherent thermoset nature of epoxy resins, defined by their densely crosslinked, three-dimensional network, renders them particularly resistant to conventional recycling methods. Unlike thermoplastics, they cannot be remelted or reprocessed without significant degradation, making end-of-life management a persistent challenge. Current recycling strategies for epoxy-based composites can be broadly classified into mechanical, thermal, and chemical approaches [56].

Mechanically recycled waste material is ground into particulate forms through grinding or milling and can be reused as filler material. While simple and cost-effective, this method typically results in materials with diminished performance and limited value-added potential [56, 57]. Thermal recycling methods, such as pyrolysis and fluidized bed processes, aim to decompose the polymer matrix at elevated temperatures (typically > 400°C), recovering inorganic fillers or fibres, particularly in fibre-reinforced composites [58]. However, these techniques often lead to the degradation of valuable reinforcing fibres and emit volatile organic compounds (VOCs), raising environmental and economic concerns. Chemical recycling is emerging as the most promising route for recovering functional value from epoxy thermosets [59]. This treatment involves breaking down the epoxy polymer network into smaller oligomers or monomers through solvolysis (e.g., glycolysis, hydrolysis, or aminolysis) or catalytic processes under controlled conditions. Chemical recycling has the potential to yield reusable feedstock or functional recyclate materials suitable for further processing. Despite its promise, the technique faces several challenges, including incomplete depolymerization, selectivity issues, and the need for precise control of reaction conditions to avoid undesirable side reactions [56, 60].

Recent advances have focused on dissolution-based depolymerization using specific solvent-catalyst systems capable of selectively cleaving crosslinks while preserving functional groups [61]. This enables partial or full recovery of matrix components, opening pathways for repurposing the recyclate into new formulations such as thermoplastics, resins, or adhesives.

The continued development of efficient and scalable chemical recycling processes is critical to closing the loop for high-performance epoxy systems and aligning their life cycle with circular economy principles.

2.3 Recycling of Epoxy Thermoset

Wu et al. developed a solvolysis process for FRCs using different mild acid solutions. With a 20% acetic acid aqueous solution they obtained a 100% of dissolution within 1 hour at 100°C. Likewise, a 1.9% HCl aqueous solution containing ethylene glycol totally dissolves the cured epoxy resin sample within 1.5 hours at 145°C. The obtained matrix residue powder was blended in different wt% with virgin epoxy resin. Hence, the matrix was re-used in second-life application. They discovered that with the addition of the recyclate powder, up to 5 wt%, the flexural and thermal properties were similar to the virgin resin. Nonetheless, increasing the wt% of powder resin was shown to decrease dramatically the above mentioned properties. Moreover, it was observed that the recyclate worked more as a filler than as a molecular component participating in the cross-linked structure [62]. An economical ad efficient strategy for chemcycling cured epoxy resin from its carbon fiber reinforced epoxy resin was proposed by Wang et al.. A 15 wt%

$AlCl£_3/CH_3COOH$ solution at 180 °C for 6 hours was used as the degradation system, where $AlCl_3$ was used to act as Lewis acid catalyst promoting the selective cleavage of the C-N bonds. The described method was evidenced by FTIR, NMR, and GPC to be successful with a recovery up to 97.43 wt% of the cured epoxy resin [16]. In all these cases the recycled epoxy matrix was never transformed into a new polymer, with good mechanical and thermal properties.

A possible application for the recycled epoxy resin was found in its use as adhesive polymer. Indeed, the strength of the adhesive joints is promoted by the presence of chemical groups that enable strong interfacial interactions.

2.4 Recyclable Epoxy Resins and Introduction to Recyclamine®

As a result of non-recyclability of traditional epoxy thermosets, the development of recyclable epoxy systems has emerged as a critical research focus in the pursuit of sustainable thermosetting polymers. Recyclable epoxies are engineered to incorporate cleavable linkages or dynamic covalent bonds within the network structure, enabling chemical depolymerization under specific conditions. These resins maintain the performance characteristics of conventional epoxies during service but can be broken down into soluble fragments or oligomers at end-of-life, allowing for material recovery and potential reprocessing.

A prominent strategy in this domain involves the use of cleavable curing agents, which are designed to introduce labile bonds, such as ester, imine, or carbamate functionalities, into the cured network [18]. These bonds can be selectively cleaved under mild chemical conditions, typically in the presence of acids, bases, or nucleophiles, without requiring extreme temperatures or compromising the quality of the recycled material.

One of the most notable developments in this area is the Recyclamine® technology, a family of patented cleavable amine-based curing agents developed by Connora Technologies. Recyclamine® hardeners are formulated to react with conventional epoxy resins, forming a fully crosslinked thermoset with properties comparable to traditional epoxy systems. However, the key innovation lies in the incorporation of degradable linkages within the hardener structure. Upon exposure to mildly acidic aqueous conditions, these linkages undergo hydrolysis, allowing the cured network to be depolymerised and dissolved [63].

The Chapter 3 introduces the Recyclamine®, and Chapter 4 explores the chemistry of the curing systems of Recyclamine® adopted in this work in greater detail, followed by an analysis of their depolymerization behaviour, recyclate characteristics. Chapter 5 presents the Recyclamine® repurposing potential in various applications.

Materials and Methods 3

3.1 Materials

The epoxy resin used was Recyclamine® 007R, and the slow-reactive hardener was Recyclamine® 013H3, both manufactured by Aditya Birla Group (ABG). Sodium hydroxide, reagent grade (≥98%) in pellets, and acetic acid 96% were purchased from Sigma-Aldrich.

3.2 Methods

3.2.1 Pre-sample preparation

To enable recycling of the epoxy matrix separated from the fibres, the process began with the manufacturing of a glass-fiber reinforced laminate, followed by depolymerization of the composite and proceeded by isolating the polymer matrix from the reinforcing fibres.

3.2.1.1 Laminate manufacturing

The laminate manufacturing followed a standard procedure commonly used for composite material fabrication within the department.

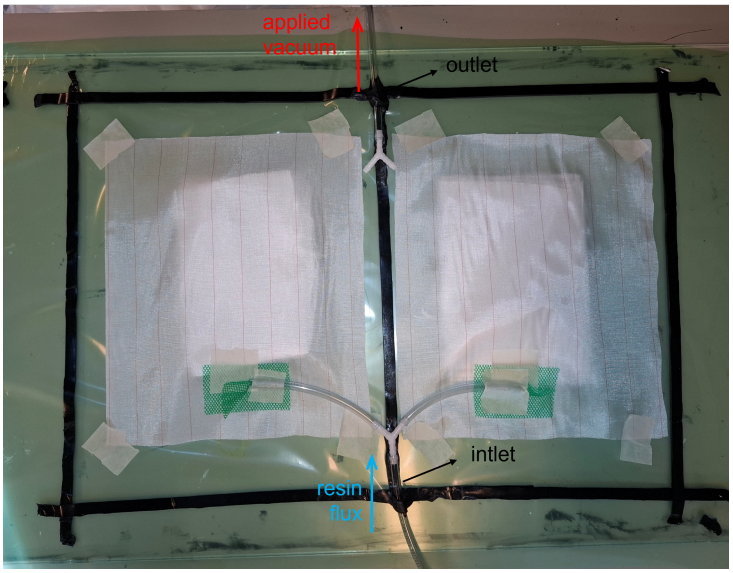

Figure 3.1: Representation of the vacuum resin infusion set up for the laminate manufacturing process.

To prepare the laminate, the fibres were placed on a vacuum foil and afterwords covered with peel ply strips. The tubes for infusing the resin were placed at the bottom of the fibres to see the flowing flux of the resin in the fibres (Figure 3.1). The system was then put under vacuum until the inner pressure reached 20 mbar. Subsequentially the vacuum chamber was inflated with a

mixture of resin and hardener which was previously mixed and then heated under vacuum at 40 °C to remove any bubbles. The laminate was then cured for 18 hours at 60 °C and post-cured for 8 hours at 80 °C.

3.2.1.2 Laminate recycling

The laminate was placed on a perforated stainless steel platform. Afterward, a 30 wt% acetic acid (AcCOOH) solution was poured in the glass bowl. The system was then heated at 80 °C while mixed at 150 rpm, until the laminate was totally dissolved, about 24 hours. The solution was measured to have a pH of about 3.

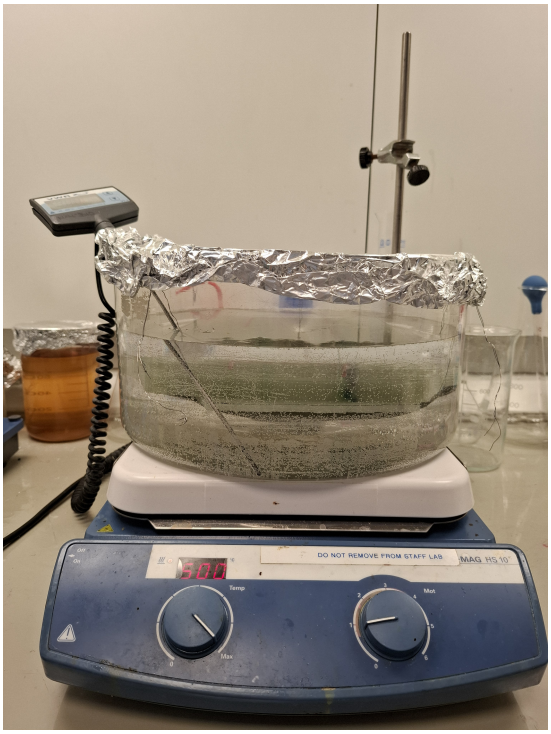

Figure 3.2: Set up for the chemical recycling process.

3.2.1.3 Precipitation

The final method employed to obtain a fine powder is detailed herein. However, as this procedure was selected following extensive experimental trials, the alternative methods explored during the optimization process are presented in Appendix A 7.

About 300 ml of recycled solution was added to 600 ml of 10% wt NaOH solution, while stirring at 250 rpm. The precipitated polymer was left stirring in the solution for 10 min to maximise the neutralization. Once the polymer was precipitated (Figure 3.3a), it was washed 8 times in deionized (DI) water (Figure 3.3b) to remove the acetic acid in the form of sodium acetate ($CH_3COO^-Na^+$), thanks to its deliquescent and hygroscopic nature. The polymer was then dried for 1 day at room temperature. Successively, to obtain a rapid and consistent reduction in particle size for subsequent analysis, the recycled polymer (RP) was ground for 10 s in a compact blade-based electric grinder equipped with two stainless steel blades and rated at 150 W. The powder was further dried for 1 day.

(a) (b)

Figure 3.3: (a) recycled polymer washed once in 10 wt% NaOH solution and then rinsed with DI water; (b) recycled polymer washed once in 10 wt% NaOH solution, then rinsed 8 times with DI water, then air dried.

3.2.1.4 Up-concentration

To enable the use of the recycled material in applications where a powder form is not suitable, such as formulations requiring a concentrated liquid phase, as the re-dissolution process demonstrates being time-consuming and inconsistent, a concentration step was necessary. The recycling solution, obtained by dissolving epoxy resin in a 30 wt% acetic acid solution, was subjected to a concentration step. To achieve this, diverse approaches have been used to up-concentrate the recycling solution:

- thermal treatment on a heating platform with continuous mixing;
- freeze-drying;
- thermal treatment in a depressurized environment;
- evaporation of thin layer in vacuum oven.

For the sake of clarities, the different approaches are described in the Chapter 4, when the corresponding results are presented.

3.2.2 Sample preparation

Two different materials were used in the production of the shear testing samples: VWR® Microscope Slides (76x25x1 mm) and an epoxy laminate reinforced with 1 plate of glass fibres, cut into samples of 90x8 mm. In the first case of material, the RS was disposed of the right amount on a 25x25 mm surface, evaporated until the chosen concentration, and then a second microscope slide was pressed on the area with a weight of 1 kg, then cured in vacuum oven at 80 °C for 24 hours. The same procedure was applied for the epoxy laminate, but the adhesive area was of 10x8 mm.

3.2.3 Fourier Transform Infrared Spectroscopy (FTIR)

The chemical structure of the received polymer is analyzed with a Nicolet iS 20 FTIR spectrometer (ThermoFisher Scientific). The spectra are recorded in the range of 4000 to 600 cm^{-1}. The

environment, which serves as background, is scanned in advance, after which samples are scanned with the same scanning range.

3.2.4 Thermogravimetric analysis (TGA)

TGA was performed with a SDT-650 TGA (TA Instruments). The recycled resin samples were heated at a rate of 10.0 $°C$/min to 700$°C$ in nitrogen atmosphere. From the thermogravimetric curves different values such as the onset of thermal degradation (T_{on}), the weight loss, and the peaks of the second derivate were obtained.

3.2.5 Differential scanning calorimetry (DSC)

DSC was performed using a DSC Q2000 (TA Instruments). The procedure chosen was a Heat/Cool/Heat method, with a heating step from $-50°C$ to $300°C$ at a constant heat rate of $10°C$/min, followed by a cooling step to $-50°C$ at a rate of $10°C$/min and a final heating scan with the same set up of the first heating step. Dynamic measurements were undertaken in a nitrogen atmosphere (50 ml/min).

3.2.6 Injection moulding

The HAAKE MiniJet II (Thermo Scientific) was used to injection moulding the recycled material. The cylinder temperature was varied to ensure the optimal temperature. The material in case of the RR/LDPE mix was left in the cylinder for 5 min to ensure the complete melting of the polymers and hence an enhanced blending. Both the injection pressure and the post pressure were of 500 bar.The mould temperature was fixed at 85 °C. In order to improve the releasing of the sample from the mould a long lasting PTFE mould release was used.

3.2.7 Tensile testing

The uniaxial tensile testing was conducted on an Instron 5944 tensile tester 2kN capacity, in accordance with ISO 527-1:2019 at a crosshead speed of 10 mm/min and at room temperature at 20 °C.. An extensometer was used to measure the elongation until a strain of 4%.

3.2.8 Characterization of adhesion ability

Adhesive lap shear testing was conducted in tension mode on two different machines. For the microscopy slide samples, it was conducted Zwick Z010 universal tensile device was used with a test speed of 50 mm/min. The epoxy laminate samples were tested on a UCT 100kN TRAM A/S device at a test speed of 10 mm/min. The lap shear strength was calculated using Eq. 3.1.

$$\text{Lap shear strength (Pa)} = \frac{\text{maximum loading force (N)}}{\text{bonding area (m}^2\text{)}} \tag{3.1}$$

3.2.9 Contact angle

A droplet of the recycling solution (RS) was deposited onto the designated surface of the epoxy laminate used for shear testing. An image of the droplet was then captured under controlled conditions. The contact angle was subsequently determined using ImageJ (Fiji distribution) by analysing the droplet profile in the captured image.

Epoxy Recyclate 4

This chapter focuses on the development and evaluation of a dissolution-driven epoxy recycling pathway utilising aqueous acetic acid solution to break down the cured network. Beginning with a structural characterisation of the initial epoxy system via FTIR spectroscopy, the study proceeds to examine the chemical behaviour of the crosslinked resin under acidic conditions, highlighting the absence of C−O−C bands in the recovered material and suggesting the lack of re-crosslinking during drying. The discussion explores the role of chemical equilibrium and thermophysical effects in this outcome. Following dissolution, neutralisation with sodium hydroxide is used to stabilise the recyclate in a chemically irreversible form, although the batch-to-batch variability, evident from FTIR anomalies such as ester carbonyl signals, suggests sensitivity to processing history and possible oxidative degradation during curing process. To expand the functional utility of the recyclate, this chapter also investigates its solubility behaviour in aqueous acetic acid medium and assesses strategies to enhance material concentration and recovery via up-concentration protocols. Ultimately, this chapter aims to lay the groundwork for advanced valorisation approaches, enabling the integration of epoxy recyclates into new thermoplastic, resin, and adhesive formulations that support circular economy principles.

4.1 Cured epoxy

The curing reaction between Recyclamine® 013H3 and DGEBA epoxy resin proceeds through a step-growth polymerisation mechanism.

As outlined in Section 2.1.3, the curing mechanism begins with the primary amine groups of Recyclamine® 013H3 acting as nucleophiles, initiating an attack on the electrophilic carbon atoms of the strained epoxide rings in the DGEBA resin. This nucleophilic ring-opening leads to the formation of β-hydroxy amine linkages and produces secondary amines, which in turn can react with additional epoxide functionalities. As the network formation progresses, the hydroxyl groups generated during the ring-opening phase engage in hydrogen bonding interactions, which further activate adjacent epoxide rings by increasing their electrophilicity. This autocatalytic behavior accelerates the crosslinking reaction, culminating in the formation of a densely crosslinked, three-dimensional thermoset architecture that imparts the resulting polymer with high rigidity and mechanical durability.

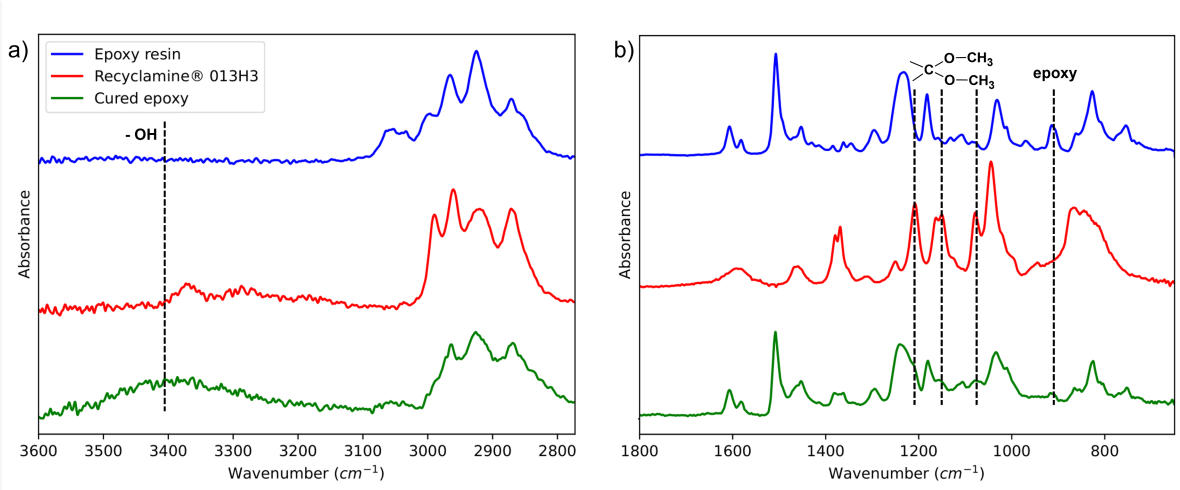

Figure 4.1: FTIR spectra of the starting components (epoxy resin - blue curve and Recyclamine® - red curve) and the resulting cured epoxy (green curve); a) enlargement of the region 3700-2700 cm^{-1}, with the peak at 3380 cm^{-1} showing the formation of hydroxyl groups from the ring-opening of the oxirane ring; b) enlargement of the fingerprint region, where the formation of katal linkage, (at 1209, 1155 and 1078 cm^{-1}) in the cured structure (green curve) and the disappearance of the epoxy group (at 913 cm^{-1}) is shown.

The FTIR spectra of the epoxy resin (blue curve), the hardener (red curve), and the resulting cured epoxy (green curve) are presented in Figure 4.1. The progression of the curing reaction is evidenced by the disappearance of the characteristic absorption band at 913 cm^{-1}, corresponding to the stretching vibration of the oxirane (epoxy) group [64], which is observed exclusively in the uncured epoxy resin. Concurrently, the emergence of a broad absorption band around 3380 cm^{-1} indicates the formation of hydroxyl groups. This feature is attributed to intermolecular hydrogen bonding interactions of the type $O-H \cdots O$, arising from the ring-opening reaction between the epoxy and amine functional groups during the curing process [65]. The absorbance peaks at 1209, 1155 and 1078 cm^{-1} are representative of the $C-O-C-O-C$ stretching vibration of the ketal linkage, present in the hardener and in the cured epoxy spectrum [66]. This central cleavable group is the key to the epoxy crosslinked networks recyclability, as it allows epoxy-based thermosets to be recycled, reused, and repurposed into epoxy thermoplastics, as described in Section 4.2.

4.2 Dissolution in acetic acid solution

The chemical structure of the polymer in the different steps of the depolymerization process was deeply analysed. Regarding the chemical reversibility of metal linkages, such as those present in the cured epoxy due to the Recyclamine® 013H3, the chemical equilibrium is governed by an acid-catalysed reaction between the ketal form and its hydrolysed products, i.e. two alcohols and a ketone, which in this case is acetone. Indeed, in the presence of aqueous acid, ketals are well known to undergo hydrolysis through a S_N1 multistep mechanism involving protonation of the ether oxygen, nucleophilic attack by water, and subsequent cleavage of the $C-O$ bond, yielding a carbonyl compound and alcohols [67, 68]. A possible equilibrium structure of the recyclate in the recycling solution, from its starting components, is reported in Figure 4.2. Here, it can be seen how during the recycling treatment, the acidic environment selectively cleaves the $C-O$ ketal bonds, leading to the formation of a poly(hydroxyaminoether) and acetone.

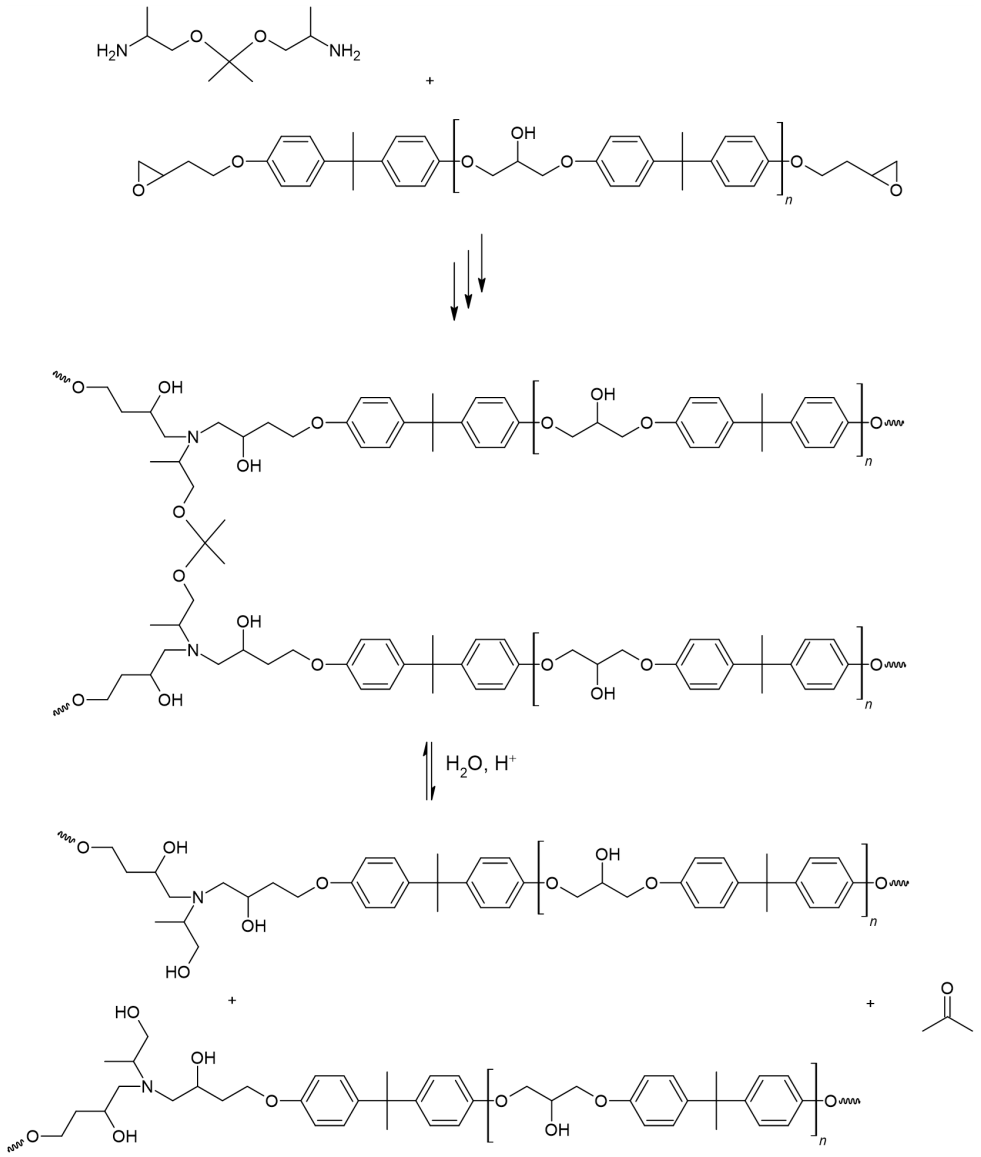

Figure 4.2: Possible formation of the equilibrium structure of the recyclate in the recycling solution, starting from its initial components.

As it is an equilibrium, it is noteworthy that this reaction is reversible. According to Le Châtelier's principle, an increase in the concentration of one of the reaction products, in this case water, will shift the equilibrium toward the formation of more hydrolysis products, thus favouring the breakdown of the ketal linkage. This result is evinced in the FTIR spectrum reported in Figure 4.3 a). Here the spectra of the cured epoxy, the recycling solution (RS) and the dried form of the RS (RS-d) are compared. The drying process would be fully explained in Section 4.3. The disappearance in the RS and RS-d spectrum of the absorbance peaks at 1209, 1155 and 1078 cm^{-1}, representative of the $C-O-C-O-C$ stretching vibration of the ketal linkage [66], means that the reaction if totally shifted towards the hydrolysed form. When water is removed from the system, Le Châtelier's principle predicts that the equilibrium will shift towards the reformation of the ketal, thereby promoting the restoration of the crosslinked polymer network. However, the FTIR spectrum of RS-d did not exhibit the reappearance of $C-O-C-O-C$ stretching vibrations, which would typically indicate the presence of ketal structures. This outcome suggests that the re-crosslinking process did not occur.

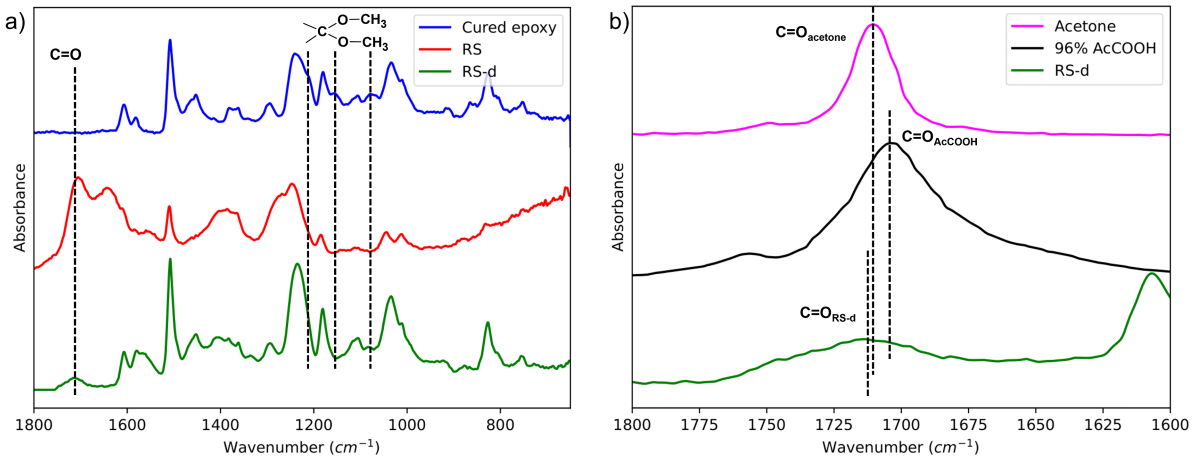

Figure 4.3: FTIR spectra of: a) the cured epoxy (blue curve), the recycling solution (RS - red curve) and the dried form of the RS (RS-d - green curve), with the peak at 1714 cm^{-1} of the carbonyl stretching vibration present in both the RS and the RS-d curves and the disappearance of the peaks at 1209, 1155 and 1078 cm^{-1} of the katal linkage in both RS and RS-d; b) the carbonyl signal of acetone, acetic acid and RS-d, showing higher coherence of the last two curves.

This discrepancy may be attributed to a combination of intrinsic chemical reactivity and macroscopic thermophysical phenomena.

On the one hand, the evaporation process may have removed not only water but also volatile carbonyl compounds, such as acetone, necessary for ketal formation, thereby preventing the reverse reaction. Nonetheless, this compositional deficit is not supported by the FTIR spectrum, where the peak at 1714 cm^{-1} of the C=O stretching vibration is still present in RS-d [66]. As illustrated in Figure 4.3 b), the carbonyl peak of the RS-d almost coincides with the acetone one, but the broadness of the carbonyl peak of acetic acid is more coherent with the shape of the peak in the RS-d spectra. In conclusion although acetone may have largely evaporated due to its high volatility, the carbonyl signal observed in the recyclate is more plausibly attributed to acetic acid molecules retained within the polymer matrix.

On the other hand, as the solution becomes more concentrated and viscous during solvent evaporation, the molecular mobility may become kinetically restricted, hindering the necessary molecular interactions for ketal reformation. Specifically, the elevated viscosity and reduced free volume of the medium significantly diminish the diffusional mobility of functional groups, such as hydroxyls and carbonyls. In this diffusion-limited regime, the possibility of effective bimolecular encounters, which are necessary for the nucleophilic attack of the hydroxyl groups on protonated carbonyl intermediates, is significantly reduced [69]. Thus, the observed presence of hydrolysed components in the dried matrix is likely to reflect a diffusion-controlled kinetic limitation, rather than a shift in equilibrium position.

4.3 Neutralization

Upon addition of the recycling solution to a 10 wt% NaOH solution, the residual acetic acid undergoes a classical acid-base neutralisation reaction with the sodium hydroxide to form sodium acetate and water. This reaction removes free protons from the system, causing the system's pH to increase markedly. Since the formation of ketals is an acid-catalysed process, the increase

in pH suppresses the catalytic action of hydronium ions required for the backward reaction to re-form the ketal linkage. Notably, ketal re-formation also requires acidic conditions, particularly for the activation of the carbonyl intermediate, and is thus impeded under basic conditions. Consequently, the sharp increase in pH effectively traps the system in its hydrolysed state by eliminating the catalytic environment necessary for re-equilibration. In this high-pH regime, the reaction becomes effectively irreversible, stabilizing the polymer in its neutralised form due to the lack of conditions required for condensation back to the ketal structure. The recyclate is washed thoroughly with water to rinse off the remaining sodium acetate resulting from the neutralization reaction alongside with the acetic acid molecules trapped in the polymer matrix. Indeed, as sodium acetate has a deliquescent and hygroscopic nature, it was possible to remove it from the recyclate, as evident from Figure 4.4.

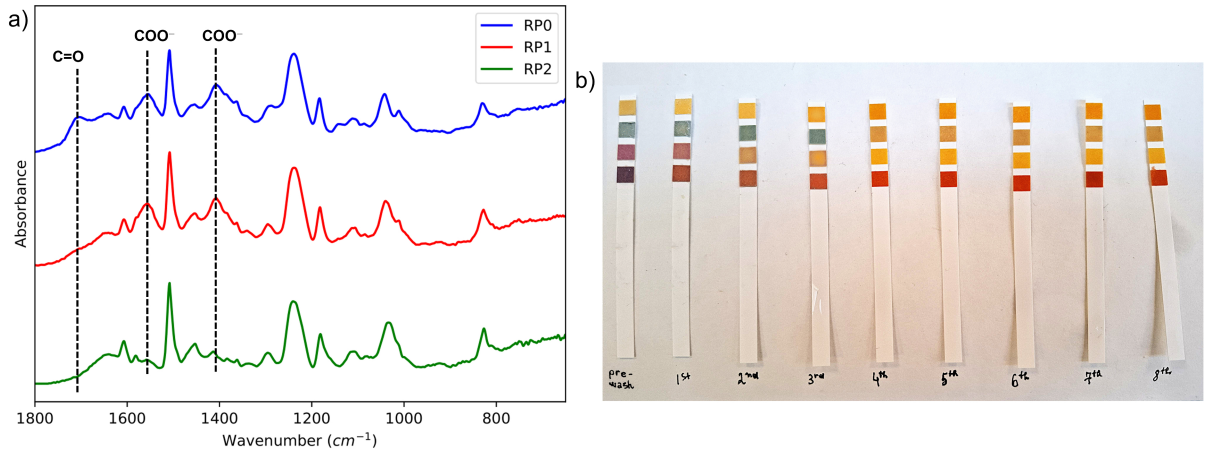

Figure 4.4: Neutralization process: a) FTIR spectra of the recyclate after precipitation process not treated (RP0), the recycled polymer washed three times in NaOH (RP1) and recyclate washed three times in NaOH and eight times in DI water (RP2). It is visible the disappearance of the peaks at 1555 and 1407 cm^{-1} in RP2, both indicating the removal of sodium acetate; b) we observe the pH reduction that is coherent with the decrease in intensity of the carbonyl peak in Figure a) and indicates the disappearance of the acetic acid molecules.

The disappearance of the peaks at 1555 and 1407 cm^{-1} (Figure 4.4 a)), corresponding to the antisymmetric and symmetric stretching vibration, respectively, of carboxylate ion COO^-, indicates that the sodium acetate, formed during the neutralization process, was successfully removed. At the same time, the gradual disappearance of the acetic acid molecules is evinced by the decrease in intensity of the carbonyl peak (Figure 4.4 a)) and the pH reduction (Figure 4.4 b)).

The FTIR spectrum of the recyclate in powder (RP-P) form is displayed in Figure 4.5, reporting the main functional groups of the obtained polymer. The broad peak at 3294 cm^{-1} is representative of the $O-H$ stretching vibration of the hydroxyl groups. The skeletal structure is defined by the peaks at 2928 and 1607, 1580, 1508, 1453 cm^{-1} related to the $C-H$ stretching vibration from the main aliphatic structure and $C=C$ stretching vibration from the aromatic ring, respectively. The asymmetric and symmetric $C-O-C$ stretching vibration of the alkyl-aryl ether bonds are identified by the peaks at 1235 and 1032 cm^{-1}, respectively [66]. The hypothetical structure of the recyclate is supported by the glass transition temperature revealed from the DSC thermogram. Indeed, the recovered polymer presents a T_g of 66.64 °C (7.13), which is chorten with the thermal behaviour described in literature for poly(hydroxyaminoethers) [70].

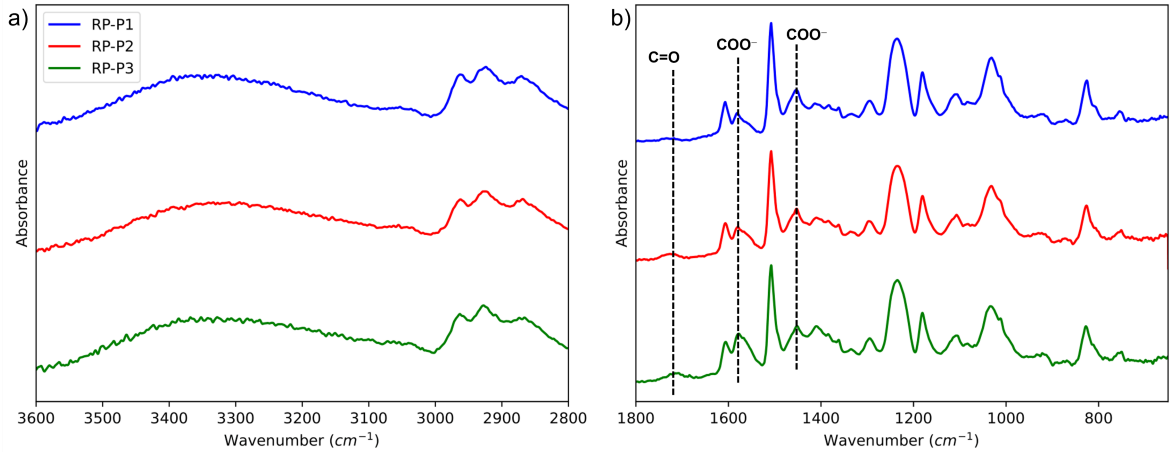

Figure 4.5: FTIR spectra of the neutralized recyclate in powder form of three samples starting from a different batch of cured epoxy: RP-P1, RP-P2, and RP-P3. The difference in the intensity of the peak at 1555 and 1407 cm^{-1}, representative of carboxylate ion COO^-.

However, the powder production process has demonstrated inconsistency. The primary distinction observed in the FTIR spectra is a higher concentration of sodium acetate traces, as indicated by the peaks at 1555 and 1407 cm^{-1}, corresponding to the antisymmetric and symmetric stretching vibration, respectively, of carboxylate ion COO^-, in Figure 4.5 b) with increased intensity. These discrepancies might be the result of differences in the curing process. Indeed, each sample (RP-P1, RP-P2, RP-P3) was produced starting from a different batch of cured epoxy. In particular, the last batch presented a minor decolourisation and a new peak appeared in the fingerprint area (Figure 4.6).
Specifically, an unexpected infrared absorption band was observed at approximately 1745 cm^{-1}, which is characteristic of an ester carbonyl stretching vibration [66, 71]. This peak is not typically present in standard epoxy-amine curing reactions, which predominantly form secondary amines and secondary alcohols (with hydroxyl groups) [72]. The appearance of this ester band can be attributed to oxidative degradation of the epoxy resin under elevated temperatures. In fact, esterification necessitates a substantial energy input. The thickness of the sample may have led to an exothermic reaction, which in turn made thermal degradation feasible. The thermal oxidation

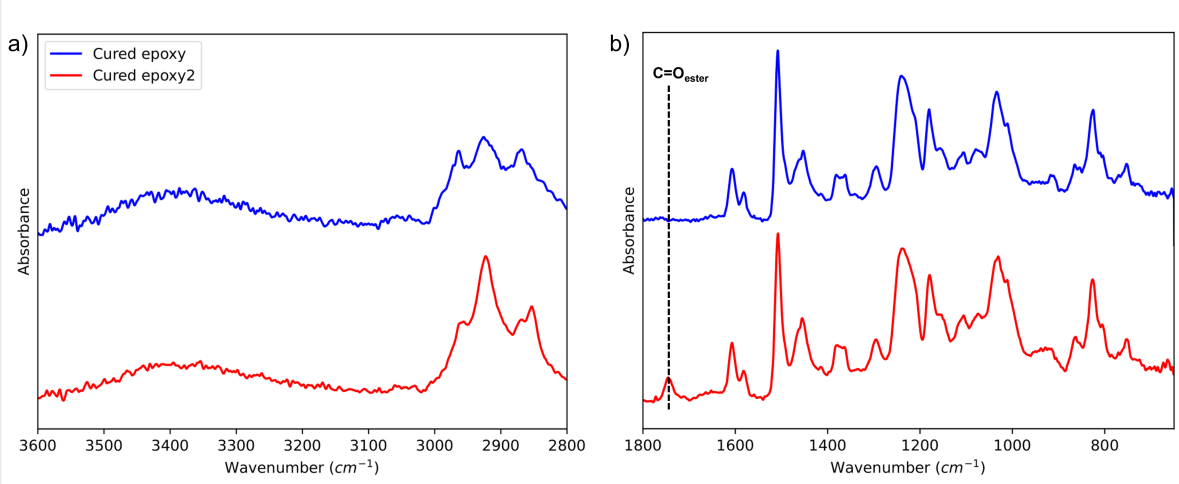

Figure 4.6: FTIR spectra of different batches of cured epoxy: in the spectrum of the Cured epoxy2 (red) is visible a non-conventional peak at 1745 cm^{-1}, characteristic of the ester carbonyl.

processes can lead to the formation of carboxylic acid groups ($R-COOH$). Concurrently, hydroxyl groups ($R'-OH$) are generated as a result of epoxide ring-opening polymerization [73]. Under heat, these carboxylic acids can undergo Fischer esterification with available hydroxyl groups, yielding ester linkages ($R-COO-R'$) and water as a byproduct [74]. The absence of water signals in the FTIR spectrum is consistent with its evaporation during the thermal process. The presence of the ester carbonyl peak suggests that oxidative degradation and subsequent esterification reactions occurred during curing, leading to ester incorporation within the polymer network. This can contribute to reduced solubilization, as the formation of ester linkages can increase the crosslinking density of the polymer network, leading to decreased solubility [75].

4.4 Solubilization of recycled polymer in acetic acid solution

The recycled polymer powder was dissolved in a 30%wt aqueous acetic acid solution in different w/v ratios (Figure 4.7). The viscosity was controlled during the process to define the application of the final products.

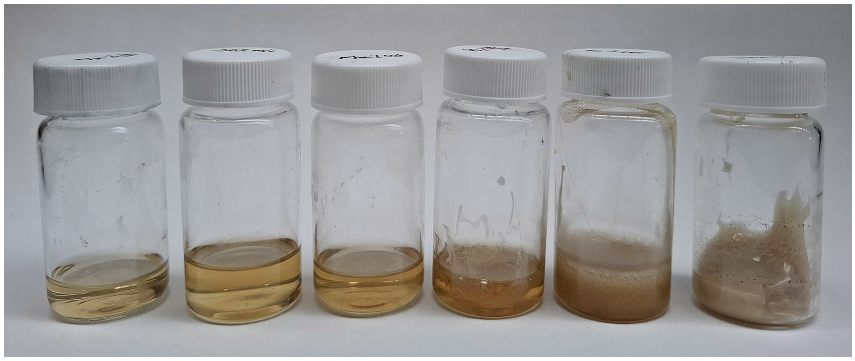

Figure 4.7: Different % w/v RP-P1 solution in 30% wt acetic acid solution. From left to right a) 15% w/v, b) 30% w/v, c) 50% w/v, d) 70% w/v, e) 90% w/v and h) 100% w/v.

This procedure was repeated with all the PR-P produced, showing different results. The RP solution in 30% wt AcCOOH obtained by using the recyclate powder from the third batch (PR-P2), showed an improved miscibility. The steps to arrive to a 95% w/v RP solution are reported in Figure 7.10.

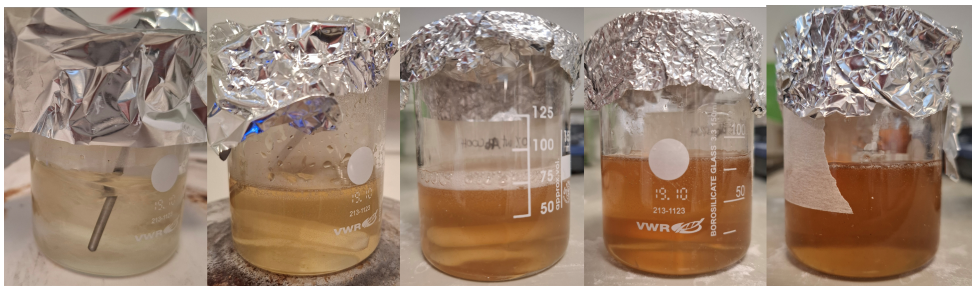

Figure 4.8: Different steps of the RP in 30% wt acetic acid solution preparation. From left to right a) 15% w/v, b) 30% w/v, c) 50% w/v, d) 90% w/v and e) 95% w/v.

The presence of acetic acid molecules in the polymer structure function as an emulsifier when the polymer is added in the 30% wt AcCOOH solution. Indeed, the hydrophilic -COOH end groups of the AcCOOH molecules strongly interact with water molecules via hydrogen bonding and electrostatic interactions. Whereas, the hydrophobic -CH_3 end groups have less affinity for water and may preferentially associate with nonpolar regions, such as the polymer powder surface.

This would increase the solubility of the RP powder compared to the RP powder obtained in the second batch (Section 7). Here, hydrophobic interactions, arisen from the disposition of non-polar hydrophobic polymer molecules to cluster together in water in order to decrease the overall interfacial area between the water molecules and the hydrophobic end groups, inhibit the dissolution of the RP powder in the AcCOOH solution. These considerations are supported by the visual difference between the 90% w/v RP solution showed in Figure 4.7 and the 95% w/v RP solution displayed in Figure 7.10. The higher clarity of this lastly produced solution is a symbol of the greater ability of water molecules to dissolve the RP powder particles.

Nevertheless, the PR-P3 appeared in not being soluble at all, resulting in a two-phase system. This unexpected result, might be related to the differences in the starting material, and to a greater presence of impurities in the form of sodium acetate as evinced in the spectrum in Figure 4.5 b).

The powder production process has demonstrated inconsistency, specifically by yielding insoluble powder in a 30% acetic acid solution, resulting in a two-phase system, as demonstrated in Section 4.3 and 4.4. In addition to this inconsistency, the procedure for obtaining the dry polymer and then dissolve it in an aqueous solution of acetic acid presented long processing times. Consequently, a more reliable, consistent, and time-efficient glue production process has been identified, which produces a concentrated RP solution in the acetic acid solution, as described in the following section.

4.5 Up-concentration of recycling solution

As discussed in Section 3.2.1.4, to increase the recycling solution concentration, several approaches have been used, which are presented here together with their results.

As first approach, the solution underwent thermal treatment. A small volume was transferred into a 50 mm diameter beaker and heated at 40 °C while stirring at 1000 rpm for 21 hours and 30 minutes. The weight of the solution was monitored hourly during the initial five hours of treatment. This process resulted in a total weight loss of 51.66%, corresponding to a final polymer solution concentration of approximately 62% w/v. However, the formation of a viscous surface film was observed, indicating that the evaporation process may have been hindered by the development of a diffusion barrier or a skin layer at the air-liquid interface. Moreover, due to its lower boiling point, water molecules will evaporate first increasing the acetic acid concentration of the solution. This could induce chemical degradation to the polymer structure.

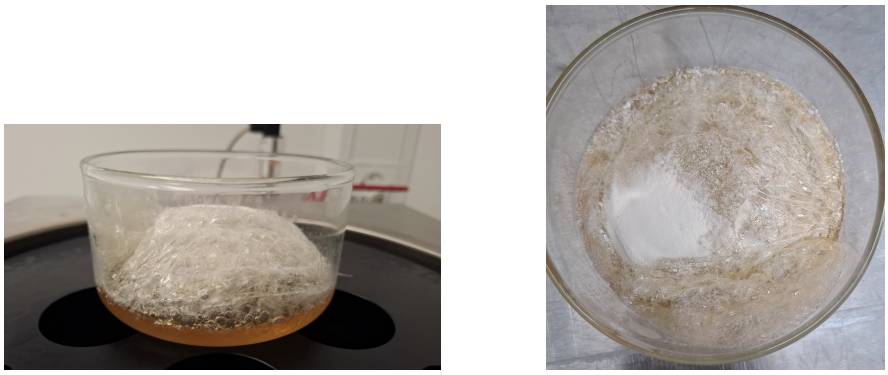

(a) (b)

Figure 4.9: The dome-like structure formation at the surface of the solution after the freeze-dried solution (at -50 °C for 18 hours).

To avoid these problems the recycling solution was freeze-dried at -50 °C for 18 hours. Nonetheless, this procedure also presented problems. A distinct dome-like structure was formed at the surface of the solution, as observable in Figure 4.9. This phenomenon is attributed to rapid surface sublimation together with a possible phase separation between water and acetic acid molecules occurring during the freezing step. The semi-riding film at the liquid-air interface, likely due to the acetic acid crystallization and polymer-rich gelation, acted as a barrier trapping sublimated vapours, resulting in an incomplete solvent removal, as demonstrated by the residual solution at the bottom.

Figure 4.10: The pressure container for up-concentrating the solution under vacuum.

Owing to the ineffectiveness of the freeze-drying approach, subsequently, a pressure container was used to put the recycling solution under vacuum (see Figure 4.10). The pressure container had inside a beaker where the recycling solution was deposited, and depressurized. The whole system of the pressure container was then heated at 40 °C over night. However, no significant changes were experienced, probably due to the lack of internal system circulation, and therefore, the liquid could not evaporate and exit. Further, the problem of the formation of a thick film at the interface (see above) was still present.

Ultimately, the primary challenge in up-concentrating the solution was identified as the diffusion of solvent molecules through the polymer matrix. The final strategy involved reducing the recycling solution layer's thickness and directly applying it to the specimen surface. Indeed, spreading a small amount of polymeric solution into a thin layer with a large surface area would lead to faster and more uniform evaporation, especially in a vacuum oven where surface evaporation is already enhanced. The optimal set up was found to be adding 0.19 g of RS on a 2.5x2.5cm area of the specimen and dry it under vacuum at 20 mbar for 8 min at 60 °C. This procedure guarantees a weight loss of about 63%, with an increase in concentration up to about 93.8% w/v, still keeping the polymer solution sufficiently "wet" to ensure a good adhesion. The samples for shear testing were prepared by placing the concentrated RP solution between two microscope slides, followed by the application of a 1 kg load to ensure uniform distribution. Subsequently, the samples were cured under vacuum conditions at 20 mbar and a temperature of 80 °C for 24 h.

4.6 Conclusion

The research presented in this chapter confirms the technical feasibility of recovering functional recyclates from cured epoxy networks through an acetic acid-based dissolution process. The FTIR spectra of the depolymerized material reveal clear changes in chemical structure, notably the absence of key katal linkages. These findings underscore both the chemical potential of mild-acid depolymerization and the susceptibility of the epoxy backbone to thermal and oxidative pathways during processing. Neutralization in a basic medium provides a promising route to stabilize the recovered product, but process consistency remains an issue due to batch variability in feedstock and reaction dynamics. The solubilization experiments further demonstrated the recyclate's chemical adaptability, paving the way for functional reuse. However, given the observed solubility fluctuations, the up-concentration step was necessary to improve reproducibility and facilitate downstream processing. Collectively, these results suggest that epoxy recyclates possess significant material value, which can be unlocked through tailored processing strategies.

Application 5

The transition to a circular economy in polymer science demands not only efficient recycling strategies but also viable pathways for re-integrating recycled materials into high-value applications. In the case of epoxy thermosets, the recovery of functional recyclates offers a promising starting point; however, the true sustainability of such systems ultimately hinges on their valorisation potential, that is: their ability to be transformed into new, functional materials. This chapter explores the post-recovery utility of the recycled epoxy resin (RP) derived via dissolution and neutralisation, assessing its performance across multiple application domains. Section 5.1 evaluates the mechanical behaviour of an RP-low-density polyethylene (LDPE) blend. The results, interpreted via tensile stress-strain curves, demonstrate a compromised mechanical integrity, reflecting interfacial incompatibilities and poor phase dispersion. Section 5.2 addresses the chemical and rheological compatibility of RP with virgin epoxy formulations. Although the structural similarity between RP and diglycidyl ether of bisphenol A (DGEBA)-based resins suggests miscibility, RP's insolubility in the monomer matrix and its inability to undergo curing with conventional amine hardeners. The most promising outcome arises in Section 5.3, which investigates the use of RP as a structural adhesive. Thermogravimetric analysis (TGA) reveals that the RP-based solution (RS-d) retains residual moisture, contradicting visual observations, thus impacting curing efficiency and mechanical behavior. Lap shear adhesion tests demonstrate satisfactory adhesion on smooth glass surfaces, likely due to hydrogen bonding between the hydroxyl-functionalized recyclate and silanol groups on the glass. However, surprisingly, rough surfaces underperform, suggesting that mechanical interlocking is not the dominant adhesion mechanism. Contact angle analysis supports this interpretation: the low value (33°) reflects favourable wettability, enhancing chemical but not necessarily mechanical adhesion.

5.1 Thermoplastic recyclate

The recycled polymer powder was tested as thermoplastic polymer. By using the Thermo Scientific HAAKE MiniJet II dog bone tensile test samples were moulded. In case of a 100% RP the sample was glassy and extremely brittle, making it not possible to handle without breaking it (Figure 5.1). Afterwards, the recycled polymer was mixed with LDPE powder in a 50/50% wt ratio. The powder mix was moulded at different temperatures to improve the miscibility between RP and LDPE. As evinced from Figure 5.1, the increase in temperature and the lengthening of the permanence of the powder mix in the cylinder, before analysis, refined the blending. Indeed, the dog-bone sample produced at 130 °C (RP-LDPE_130) showed poor compatibility, whereas at 160 °C, and 5 min of resting in the cylinder before the moulding, the sample (RP-LDPE_160) resulted being quite homogeneous. For this reason the RP-LDPE_160 was chosen for further analysis and thus indicated simply as RP-LDPE.

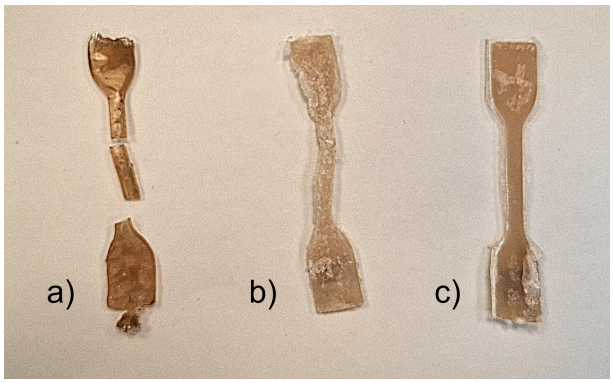

Figure 5.1: Dog bone specimens obtained by injection moulding from left to right a) 100% RP powder, b) 50%-50% RP-LDPE_130 powder (130 °C) and c) 50%-50% RP-LDPE_160 powder (160 °C).

Afterwards, a tensile analysis was performed on the 50-50% RP-LDPE sample. As reference a 100% LDPE sample was also moulded with the same parameters used for the 50-50% RP-LDPE. The 50-50% RP-LDPE sample showed a brittle behaviour, without a significant elongation (Figure 5.2 b)).

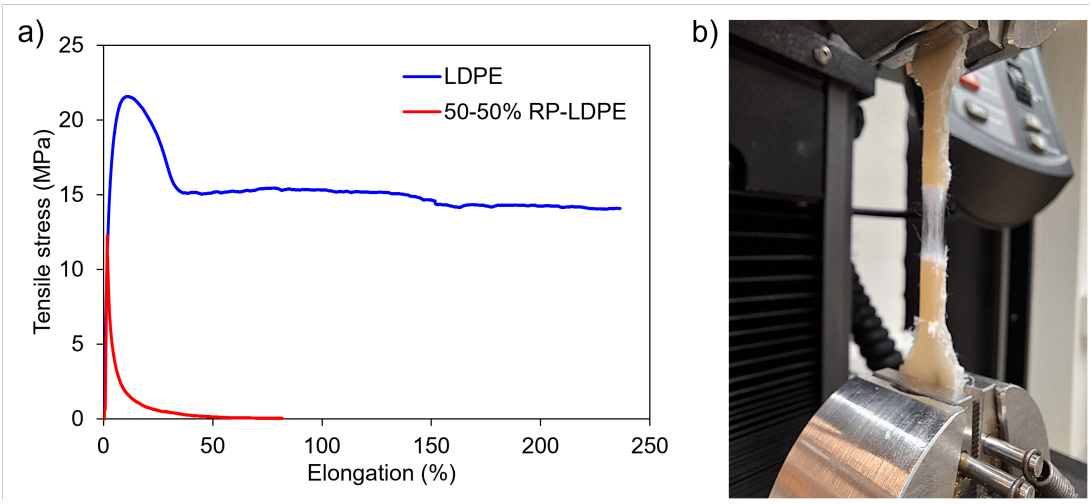

Figure 5.2: a) Stress-strain curves of LDPE sample and of the 50-50% RP-LDPE blend; b) Elongation of the 50%-50% LDPE-RP powder sample obtained during the tensile test.

The stress-strain curves of the 50-50% RP-LDPE blend revealed a significant reduction in mechanical performance compared to pure LDPE (Figure 5.2 a)). The material exhibited a low peak tensile strength of 12.38 MPa, indicating that the incorporation of the RP powder weakens the blend. This decrease in tensile strength is likely due to the poor properties of the recycled polymer, along with a possible low interfacial adhesion between RP and LDPE, which prevents effective stress transfer. The low compatibility between the two polymers is further supported by the presence of an external "coating" of more ductile material, which increased the elongation at break of the blend from 1.33% (i.e. the elongation at the maximum strength) to above 80% (see Figure 5.2 a)). Nonetheless, the core of the sample broke at 1.33% strain, highlighting the brittle nature of the material. Indeed, unlike LDPE, which undergoes extensive plastic deformation with an elongation at break the exceeds 200%, the RP-LDPE blend present a minimal plastic deformation, symbol of a drastic decline in ductility.

This behaviour is in line with the result evinced from the DSC thermogram presented in the Appendix A (7), Section A.1.3.2. Indeed, having the material such a high T_g, at room temperature

the RP sample would be in its glassy state, hence being extremely brittle and fragile. In conclusion, the performed analysis evinced the unsuitability of the recycled polymer as a thermoplastic, both pure and as a blend.

5.2 New resin

A possible re-application of the recycled polymer is to use it together with the virgin epoxy resin in the composites production. The similar chemical structure of the recycled polymer and the virgin epoxy resin should result in their miscibility. Nonetheless, the powder resulted being insoluble in the original epoxy resin, whereas the 70, 90 and 95% w/v RP solutions presented a better solubility (produced in Section 4.4). Afterwords, the 95% w/v RP solution and virgin epoxy resin were mixed in a ratio 80:20, and heated at 40 °C over night to remove the incorporated water. When cooled down the resin was mixed with the hardened in a ratio 100:28, and then poured in the mould to cure it in the oven at 80 °C for 2 days. However, the obtained product was still viscous and hence the curing process did not occur. This is coherent with the chemical structure of the RP. The curing agent did not react with the RP probably because it does not have highly reactive groups. Indeed, the reactive hardener nucleophilic molecules attach the least hindered end of the highly reactive oxirane of the virgin epoxy resin in an S_N2 reaction.

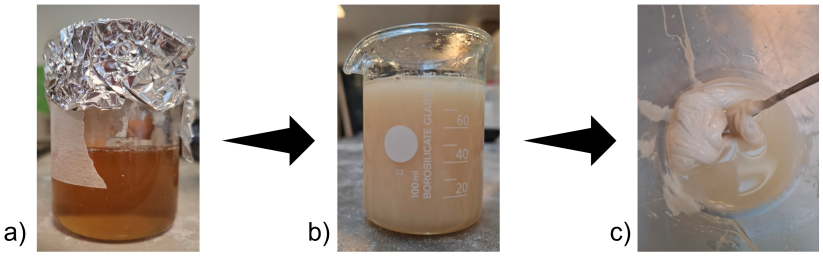

Figure 5.3: a) RP solution 95% w/v; b) RP sol. 95% w/v mixed with virgin epoxy (80:20); c) RP sol. 95% w/v + virgin epoxy mixed with the hardener.

5.3 Glue

5.3.1 Weight loss

Using TGA analysis the weight loss due to evaporation at 60 °C was evaluated. In Figure 5.4 the evaporation rate of the recycling solution (RS) and the dried recycling solution (RS-d) are reported.

Under atmospheric pressure, the solution experiences a 40.7% decrease in 30 minutes, with the reduction still in progress (as indicated by the negative slope in the diagram of Figure 5.4 a)). In contrast, when subjected to vacuum conditions at the same weight, the solution decreases by 51.2%, which is the optimal value for the intended application, within a span of 3 minutes. This demonstrate that such optimal value can be reached also at atmospheric pressure, but in longer time. Contrary to visual assumptions, RS-d is not yet completely dry. This is evidenced by the slight evaporation that is still occurring in Figure 5.4 b).

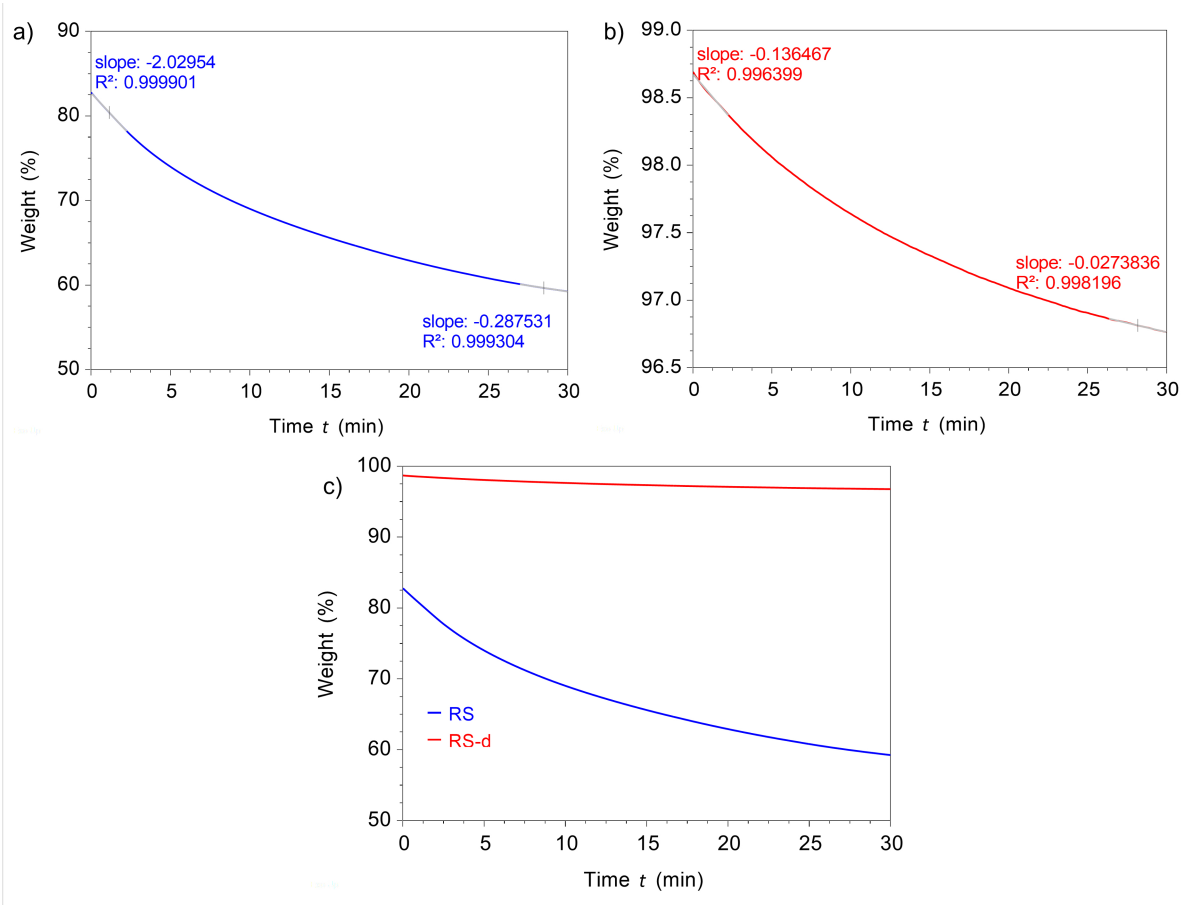

Figure 5.4: Evaporation rate of: a) the recycling solution (RS), b) the dried recycling solution (RS-d). The y-axes represent the percentage of weight lost. The curve slope and the R-squared are marked in the beginning and at the end of the curves to evidence the change; c) the two curves are presented together for better comparison.

5.3.2 Adhesion Strength of the cured recycling solution

The lap shear adhesion strength of the cured recycling solution was analysed to evaluate it's potential application as structural adhesive. The adhesion of polymers is a critical and complex phenomenon, central to a wide range of industrial applications, including automotive, aerospace, construction, and biomedical engineering. Adhesion is described as the interaction at the interface of two surfaces at the atomic and molecular levels [76]. These interactions are subject by many different factors, such as polymer chemistry, polymer physics, surface chemistry, surface physics, stress and fracture analysis. Due to the inherently low surface energy and limited presence of polar functional groups in many polymers, achieving strong adhesion properties often requires a comprehensive understanding of the underlying adhesion mechanisms. A key role in the analysis of adhesion behaviour is the characterisation of the surfaces, due to the recognised dependency on surface characteristics of the material.

The adhesion of polymer surfaces is described in literature by three main adhesion mechanisms: mechanical coupling, molecular bonding, and thermodynamic adhesion. Mechanical coupling, or mechanical interlocking, adhesive mechanism is based on the mechanical keying of the adhesive into the surface asperities [77]. On the one hand, in some cases, abrasive treatment has been observed to improve the adhesive strength and the stability of adhesive joints. On the other hand, the mechanical destruction of the surface generates macro-radicals and increases the surface area

for more chemical interactions [78]. Molecular bonding, where the strength of adhesive joints is described by the presence of intermolecular forces at the interface between the adhesive and the substrate, remains the most widely accepted explanation for polymer adhesion. The interfacial forces governing this mechanism encompass van der Waals interactions, dipole-dipole interactions, and chemical bonding phenomena, including ionic and covalent linkages [79]. Thermodynamic mechanism of adhesion is based on the equilibrium process at the interface between two materials, focusing on minimizing the interfacial tension rather than requiring specific molecular interactions [80]. It considers the surface free energy of the materials, with good adhesion occurring when interfacial tension is minimized, especially between a polymer surface and a polar substance. Young's and Dupré's equations relate surface tensions and contact angles to calculate the work of adhesion. Various theories, such as Fowkes' dispersion and polar components, geometric mean approaches, acid-base theory, and equation of state models, provide methods to quantify surface free energy and predict adhesion behavior. This mechanism highlights the importance of surface energy and wettability in adhesion, although real surfaces' roughness and chemical heterogeneity can complicate the application of these models.

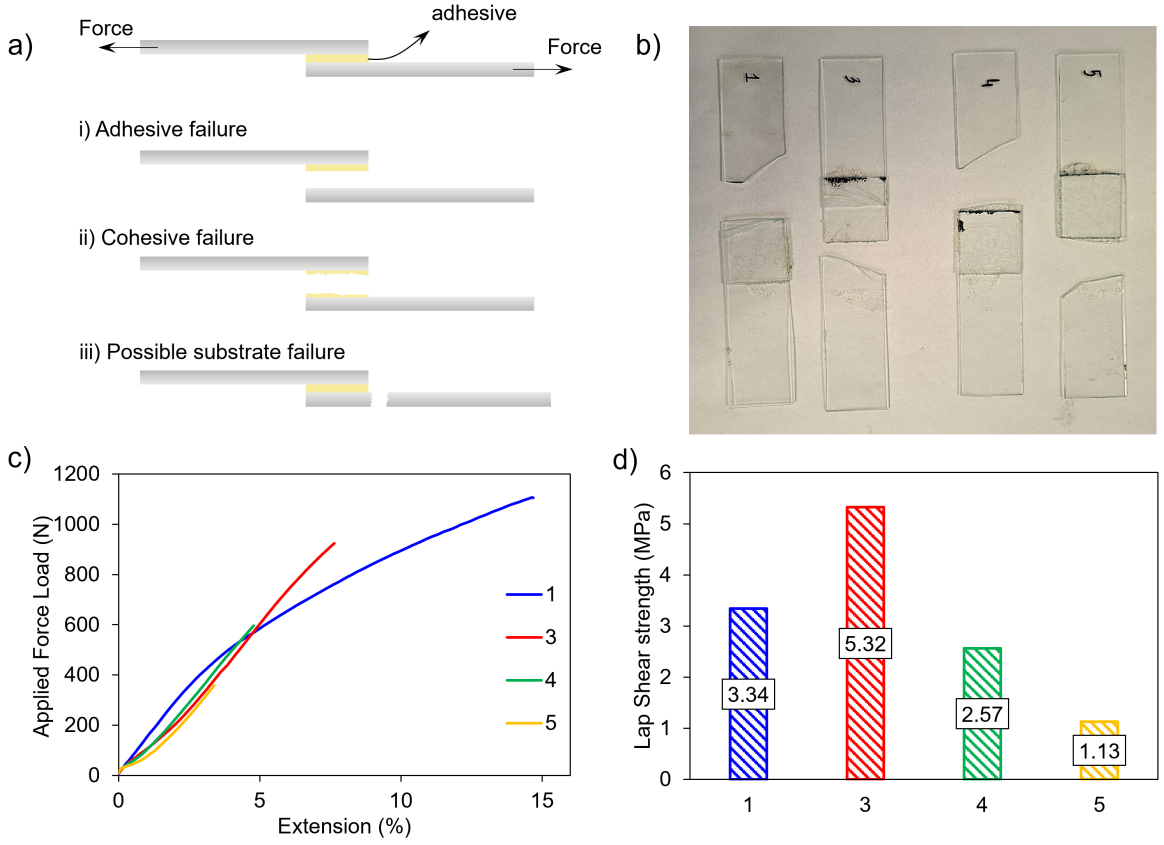

Figure 5.5: Test on the adhesive strength on microscopy slides specimens: a) the diagram of the phenomenon and of the types of failures - in this case, iii) substrate failure; b) the specimens after the test; c) representative force–extension curves for an adhesive single-lap-joint made from evaporated RS; d) the respective lap shear adhesion strength.

The first test on the adhesive strength was made on the glass slide samples. The specimens were pulled to failure in one typical mode: (iii) substrate failure, indicating that the adhesion strength of the recyclate was stronger than the substrate (Figure 5.5 a)). Representative force-extension curves from adhesive single-lap-joints for these samples are shown in Figure 5.5 c). The samples failed all in the same way except for specimen number 3, which, maybe for better grip, reported

the highest lap shear adhesion strength, with a value of 5.32 MPa (Figure 5.5 d)). Indeed, where number 1,4 and 5 broke at the edge of the adhesive area, number 3 presents the adhesive area fractured in half. These results shows a good adhesive interface, probably due to the strong hydrogen interaction between the silanol groups of the glass surface and the hydroxyl groups present in the recyclate [81]. In particular, as explained in Section 4.2, the formation of -OH end group due to acid-catalysed hydrolysis of the ketal linkage generates less steric hindered available centres.

The second test on the adhesive behaviour of the recyclate was performed using a thin sheet of epoxy laminate as a substrate. The specimens were pulled to failure in two typical modes: the first mode of failure observed was adhesive failure (i), where separation occurred at the interface between the adhesive and the substrate. This suggests that the interfacial forces—such as hydrogen bonding, electrostatic interactions, van der Waals forces, or mechanical interlocking—were insufficient to withstand the applied stress. The second mode was cohesive failure (ii), in which the failure occurred within the adhesive layer itself. This indicates that the adhesive's internal molecular structure, governed by intra- and intermolecular interactions and its viscoelastic properties, was unable to resist the imposed load.

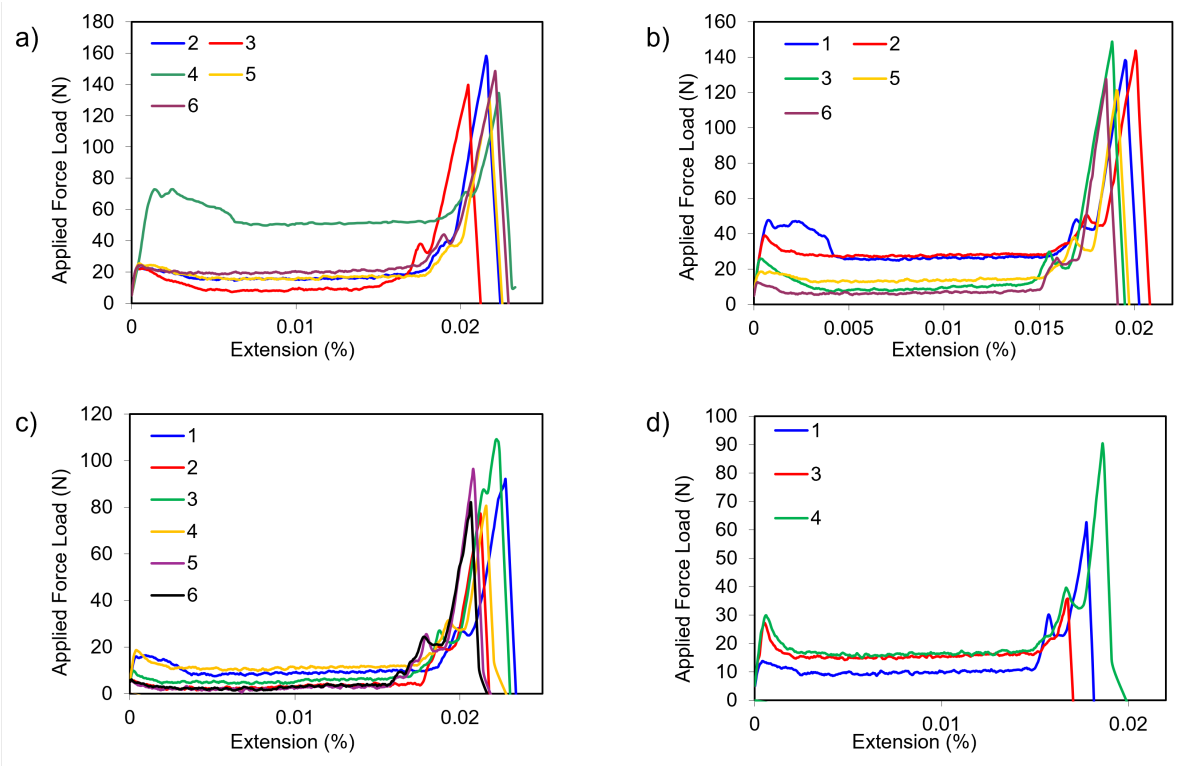

Figure 5.6: Representative force–extension curves for adhesive single-lap-joint made from RS, where: a) smooth side of epoxy laminate sample with 20 mg of RS (S20); b) smooth side of epoxy laminate sample with 60 mg of RS (S60); c) rough side of epoxy laminate sample with 20 mg of RS (R20); b) rough side of epoxy laminate sample with 60 mg of RS (R60)

As evident from Figure 5.7 a) and b), the failure mechanism is a hybrid of both mode (i) and (ii). Indeed, the shear stress-strain curve reported in Figure 5.6 present a mix behaviour. This shape of the shear stress-extension curve obtained from the recycled epoxy adhesive, exhibiting an initial peak, a plateau, and a final sharp rise, can be directly attributed to the chemistry of the recyclate and of the substrate. The formation of hydroxyl groups as result of acid-catalysed

hydrolysis is a source of hydrogen bonding, which together with physical entanglements and polar interactions is the origin for cohesion. The initial peak in the stress-extension curve corresponds to the yielding of localized domains with high physical cohesion, formed through dense hydrogen bonding networks and chain entanglements between hydroxyl-rich oligomers. Once reached the critical stress threshold, these interactions break, resulting in a localised yield and the observed peak. This initial phase is followed by a stress plateau, corresponding to a viscoelastic flow regime [82], where the relative movement of molecular chains accommodates further strain. As deformation increases, the polymer chains undergo strain-induced orientation along the deformation axis, restricting further flow and, hence, resulting in the sharp increase in stress characteristic of strain hardening before ultimate failure.

Unlikely to what expected from the mechanical interlocking mechanism, the rough side presented a lower lap shear strength with an average value of 0.99 and 0.60 MPa, for the 20 mg and 60 mg sample, respectively, against the 1.57 and 1.59 MPa of the smooth side, as shown in Figure 5.7. These are feebler than the one obtained with the microscope slides, suggesting that the interactions between adherent and substrate in this late case are weaker, probably due to a lower number of polar groups available for hydrogen bonding and other secondary interactions.

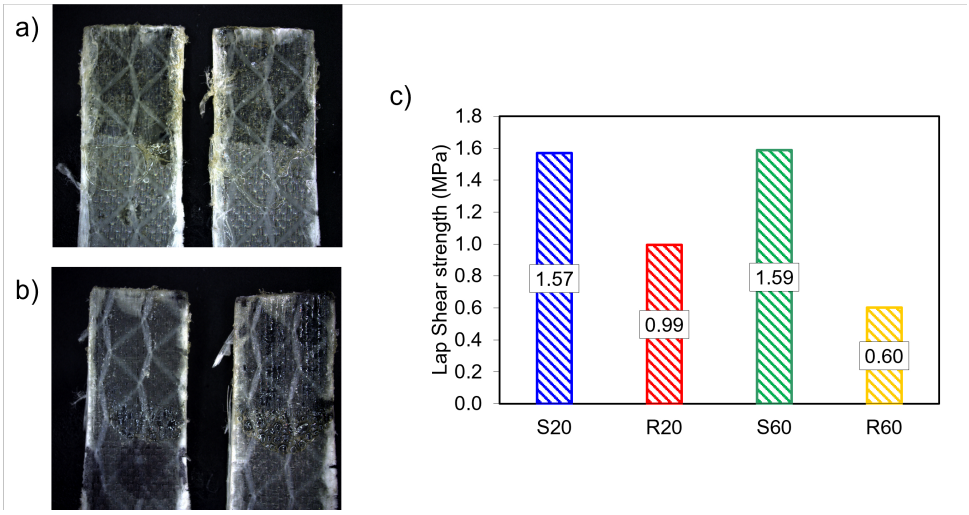

Figure 5.7: Images of the specimens after the shear test of the a) smooth side and b) of the rough side; c) the average adhesion lap shear strength values of the sample displayed in Figure 5.6.

The presented results in the first case (glass samples) give values comparable to those of instant adhesives, that are 6.2 MPa for a typical epoxy adhesive and 3.8 MPa for "instant" adhesives [83]. Instead, in the second case, they are strongly inferior.

5.3.3 Contact angle

The hypothesis of lower interaction is partially contradicted by the image in figure 5.8 where it is possible to notice a good wetting. Wettability, a key factor in adhesion, refers to how well a liquid can spread across and adhere to a surface. For an adhesive to form a strong bond, its surface energy should be lower than that of the material it is bonding to. Wettability is commonly assessed by measuring the contact angle—the smaller the angle, the better the wettability and the stronger the potential bond. In the experimental results, the contact angle is 33° for the smooth side of the epoxy laminate and 35° for the rough side, which indeed indicates a good wetting, though not complete spreading. This shows a quite strong affinity for the recycling

solution with the solid surface, even if the solution is not superhydrophilic (which would imply a contact angle close to 0°), but it is well within the hydrophilic regime.

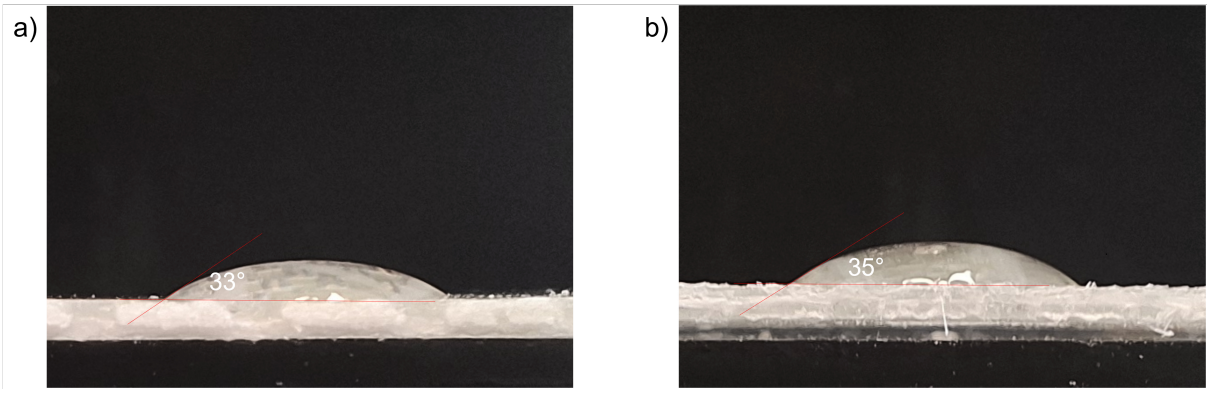

Figure 5.8: Wetting test between epoxy laminates and the RS: photo of resin spreading a) on the smooth side, with a contact angle of 33°; b)on the rough side, with a contact angle of 35°;.

5.4 Conclusion and Future Applications

The comprehensive assessment of the recyclate's applicability reveals a nuanced picture: while direct reuse in thermoplastic or epoxy resin formulations is limited by solubility and reactivity constraints, significant promise lies in adhesive and interfacial applications. The recyclate's polar functional groups enable strong secondary bonding interactions, as demonstrated in adhesive testing, and its wettability profile is favorable for coating and interface bonding scenarios. These results align with current literature advocating for function-focused polymer upcycling, wherein the chemical nature of recycled materials guides their reuse in roles that exploit rather than fight their altered structure. However, key challenges remain, particularly in batch reproducibility, moisture control, and mechanical enhancement.

In addition to its use in solution form, the RP powder was also explored as a potential binder in the production of composites materials. Binders in composites play a critical role in keeping the reinforcing components bonded together as well as distributing stress across the material. Their mechanical, chemical, and thermal properties significantly influence the overall performance and durability of the composite. In this regard, RP powder was tested between two microscope slides and heated at 80 °C for 4 hours under pressure. The produced samples were then pulled apart to qualitatively define the adhesion properties of the RP and their possible use as a binder.

Taken together, these results suggest that RP is most effectively redeployed not as a structural matrix or reinforcing resin but as a functional adhesive or binder within hybrid material systems.

Conclusion and Outlook 6

The present work has addressed a critical gap in the sustainable management of thermoset polymers, specifically focusing on epoxy-based systems, which have historically been considered unrecyclable due to their permanent crosslinked structures. Through an acid-catalysed hydrolysis strategy, this thesis has demonstrated the feasibility of chemically reclaiming a functional recyclate from cured epoxy networks. The study successfully addressed key challenges in epoxy recycling (monomer recovery, reactivity control, and reuse potential) paving the way for circular use models of high-performance thermosets.

The initial chapters detailed the molecular basis of epoxy resin systems, including the formation of epoxy monomers, resin classifications, and the curing chemistry essential to their thermal and mechanical stability. This foundational understanding was instrumental in evaluating the depolymerisation mechanism under acidic conditions. In the experimental phase, acetic acid was employed to achieve partial depolymerization of a cured epoxy resin. The absence of $C-O-C$ asymmetric stretching in the FTIR spectra of the recyclate, alongside changes observed upon neutralization with NaOH, suggested that re-crosslinking was inhibited, likely due to irreversible hydrolysis and impediment in molecular diffusion. Importantly, the process showed batch-dependent variability, highlighting the influence of thermal history and potential side reactions (such as esterification and oxidation) on recyclate chemistry. In exploring reuse strategies, the recyclate demonstrated limited compatibility with thermoplastics and virgin epoxy formulations, showing reduced mechanical integrity and inadequate cure behaviour. However, as a structural adhesive, the recyclate exhibited favourable interfacial interactions, particularly on smooth glass surfaces, attributable to hydrogen bonding. Whereas, on epoxy laminate, even though presenting a good wettability, the lap adhesion strength was quite dissatisfying. Nevertheless, these findings emphasise that reuse pathways, especially those leveraging surface chemistry and polarity, are more promising than bulk material reincorporation.

This thesis sets the foundation for a broader vision of epoxy thermoset circularity, but also reveals the complex chemical, physical, and application-driven constraints that remain unresolved. Future research should focus on the following directions:

- The observed batch inconsistencies suggest the need for real-time reaction monitoring, controlled thermal profiles, and reproducible process parameters to ensure industrial viability.
- Given the recyclate's polar functionality and surface activity, future valorisation could focus on its role as a reactive binder, compatibiliser, or interface modifier in composite systems. Here, compatibility with fibre reinforcements, ceramic substrates, or other polymers must be investigated through rheological, thermal, and mechanical analyses.

To summarize, this thesis demonstrates that, while epoxy thermosets pose significant recycling challenges, targeted chemical strategies and application valorisation can overcome many of these barriers, contributing to a future where thermosets are no longer single-use materials but integral elements in a circular economy.

Bibliography

[1] R. C. Thompson, S. H. Swan, C. J. Moore, and F. S. Vom Saal, *Our plastic age*, 2009.

[2] P. Europe. "Plastics – the fast facts 2023." (2023), Available: `https://plasticseurope.org/wp-content/uploads/2023/10/Plasticsthefastfacts2023-1.pdf`.

[3] R. Geyer, J. R. Jambeck, and K. L. Law, "Production, use, and fate of all plastics ever made," *Science advances*, vol. 3, no. 7, e1700782, 2017.

[4] X. Zhao, Y. Long, S. Xu, X. Liu, L. Chen, and Y.-Z. Wang, "Recovery of epoxy thermosets and their composites," *Materials Today*, vol. 64, pp. 72–97, 2023.

[5] C. Jehanno and H. Sardon, *Dynamic polymer network points the way to truly recyclable plastics*, 2019.

[6] F.-L. Jin, X. Li, and S.-J. Park, "Synthesis and application of epoxy resins: A review," *Journal of industrial and engineering chemistry*, vol. 29, pp. 1–11, 2015.

[7] V. H. Pham *et al.*, "Synthesis of epoxy encapsulated organoclay nanocomposite latex via phase inversion emulsification and its gas barrier property," *Journal of Industrial and Engineering Chemistry*, vol. 20, no. 1, pp. 108–112, 2014.

[8] C. Podara *et al.*, "Recent trends of recycling and upcycling of polymers and composites: A comprehensive review," *Recycling*, vol. 9, no. 3, p. 37, 2024.

[9] K. Larsen, "Recycling wind turbine blades," *Renewable energy focus*, vol. 9, no. 7, pp. 70–73, 2009.

[10] P. Deeney *et al.*, "End-of-life alternatives for wind turbine blades: Sustainability indices based on the un sustainable development goals," *Resources, Conservation and Recycling*, vol. 171, p. 105 642, 2021.

[11] P. Johst *et al.*, "Identification and environmental assessments for different scenarios of repurposed decommissioned wind turbine blades," *Materials Circular Economy*, vol. 5, no. 1, p. 13, 2023.

[12] P. Johst *et al.*, "Concept and life cycle assessment of a tiny house made from root section structures of a decommissioned large-scale wind turbine blade as a repurposed application," *Materials Circular Economy*, vol. 6, no. 1, p. 5, 2024.

[13] P. Liu and C. Y. Barlow, "Wind turbine blade waste in 2050," *Waste Management*, vol. 62, pp. 229–240, 2017.

[14] S. J. Pickering, "Recycling technologies for thermoset composite materials—current status," *Composites Part A: applied science and manufacturing*, vol. 37, no. 8, pp. 1206–1215, 2006.

[15] G. Oliveux, L. O. Dandy, and G. A. Leeke, "Current status of recycling of fibre reinforced polymers: Review of technologies, reuse and resulting properties," *Progress in materials science*, vol. 72, pp. 61–99, 2015.

[16] Y. Wang *et al.*, "Chemical recycling of carbon fiber reinforced epoxy resin composites via selective cleavage of the carbon–nitrogen bond," *ACS Sustainable Chemistry & Engineering*, vol. 3, no. 12, pp. 3332–3337, 2015.

[17] F. Tian *et al.*, "Energy-efficient conversion of amine-cured epoxy resins into functional chemicals based on swelling-induced nanopores," *ACS Sustainable Chemistry & Engineering*, vol. 8, no. 5, pp. 2226–2235, 2020.

[18] P. K. Dubey, S. K. Mahanth, and A. Dixit, "Recyclamine®–novel amine building blocks for a sustainable world," *SAMPE neXus Proceedings*, vol. 29, 2021.

[19] H. Q. Pham and M. J. Marks, "Epoxy resins," *Ullmann's Encyclopedia of Industrial Chemistry*, 2000.

[20] C. May, *Epoxy resins: chemistry and technology*. Routledge, 2018.

[21] A. Shundo, S. Yamamoto, and K. Tanaka, "Network formation and physical properties of epoxy resins for future practical applications," *Jacs Au*, vol. 2, no. 7, pp. 1522–1542, 2022.

[22] Y. Valadbeigi, "Proton affinities and gas phase basicities of epoxides and episulfides: Exceptional superbasicity of compounds with oxygen and sulfur sites," *International Journal of Mass Spectrometry*, vol. 431, pp. 63–69, 2018.

[23] H. Lee and K. Neville, *Handbook of epoxy resins*. McGraw-Hill, Incorporated, 1967.

[24] B. Ellis *et al.*, *Chemistry and technology of epoxy resins*. Springer, 1993.

[25] M. M. B. Bump, "The effect of chemistry and network structure on morphological and mechanical properties of diepoxide precursors and poly (hydroxyethers)," Ph.D. dissertation, Virginia Polytechnic Institute and State University, 2001.

[26] M. G. González, J. C. Cabanelas, and J. Baselga, "Applications of ftir on epoxy resins-identification, monitoring the curing process, phase separation and water uptake," *Infrared spectroscopy-materials science, engineering and technology*, vol. 2, pp. 261–284, 2012.

[27] N. Karak, "Overview of epoxies and their thermosets," in *Sustainable epoxy thermosets and nanocomposites*, ACS Publications, 2021, pp. 1–36.

[28] R.-M. Wang, S.-R. Zheng, and Y.-P. Zheng, "3 - matrix materials," in *Polymer Matrix Composites and Technology*, ser. Woodhead Publishing Series in Composites Science and Engineering, R.-M. Wang, S.-R. Zheng, and Y.-P. Zheng, Eds., Woodhead Publishing, 2011, pp. 101–548, ISBN: 978-0-85709-221-2. DOI: https://doi.org/10.1533/9780857092229.1.101. Available: https://www.sciencedirect.com/science/article/pii/B9780857092212500035.

[29] E. H. Farmer, "Peroxidation in relation to olefinic structure," *Transactions of the Faraday Society*, vol. 42, pp. 228–236, 1946.

[30] I. Karlsson *et al.*, "Nature-derived epoxy resin monomers with reduced sensitizing capacity-isosorbide-based bis-epoxides," *Chemical Research in Toxicology*, vol. 36, no. 2, pp. 281–290, 2023.

[31] J. C. Capricho, B. Fox, and N. Hameed, "Multifunctionality in epoxy resins," *Polymer Reviews*, vol. 60, no. 1, pp. 1–41, 2020.

[32] K. S. Meenakshi and E. P. J. Sudhan, "Development of novel tgddm epoxy nanocomposites for aerospace and high performance applications–study of their thermal and electrical behaviour," *Arabian Journal of Chemistry*, vol. 9, no. 1, pp. 79–85, 2016.

[33] X. Tang, Y. Zhou, and M. Peng, "Green preparation of epoxy/graphene oxide nanocomposites using a glycidylamine epoxy resin as the surface modifier and phase transfer agent of graphene oxide," *ACS applied materials & interfaces*, vol. 8, no. 3, pp. 1854–1866, 2016.

[34] N. R. Paluvai, S. Mohanty, and S. Nayak, "Synthesis and modifications of epoxy resins and their composites: A review," *Polymer-Plastics Technology and Engineering*, vol. 53, no. 16, pp. 1723–1758, 2014.

[35] C. Ding and A. S. Matharu, "Recent developments on biobased curing agents: A review of their preparation and use," *ACS Sustainable Chemistry & Engineering*, vol. 2, no. 10, pp. 2217–2236, 2014.

[36] T. Vidil, F. Tournilhac, S. Musso, A. Robisson, and L. Leibler, "Control of reactions and network structures of epoxy thermosets," *Progress in Polymer Science*, vol. 62, pp. 126–179, 2016.

[37] N. Bouillon, J.-P. Pascault, and L. Tighzert, "Epoxy prepolymers cured with boron trifluoride-amine complexes, 1. influence of the amine on the curing window," *Die Makromolekulare Chemie: Macromolecular Chemistry and Physics*, vol. 191, no. 6, pp. 1403–1416, 1990.

[38] J. V. Crivello and J. Lam, "Diaryliodonium salts. a new class of photoinitiators for cationic polymerization," *Macromolecules*, vol. 10, no. 6, pp. 1307–1315, 1977.

[39] J. V. Crivello and J. Lam, "Photoinitiated cationic polymerization with triarylsulfonium salts," *Journal of Polymer Science: Polymer Chemistry Edition*, vol. 17, no. 4, pp. 977–999, 1979.

[40] K. Takuma, T. Takata, and T. Endo, "Cationic polymerization of epoxide with benzyl phosphonium salts as the latent thermal initiator," *Macromolecules*, vol. 26, no. 4, pp. 862–863, 1993.

[41] M. Heise and G. Martin, "Curing mechanism and thermal properties of epoxy-imidazole systems," *Macromolecules*, vol. 22, no. 1, pp. 99–104, 1989.

[42] V. Jíšová, "Curing mechanism of epoxides by imidazoles," *Journal of Applied Polymer Science*, vol. 34, no. 7, pp. 2547–2558, 1987.

[43] L. Matějka, S. Pokorný, and K. Dušek, "Acid curing of epoxy resins. a comparison between the polymerization of diepoxide-diacid and monoepoxide-cyclic anhydride systems," *Die Makromolekulare Chemie: Macromolecular Chemistry and Physics*, vol. 186, no. 10, pp. 2025–2036, 1985.

[44] X. Fernàndez-Francos, X. Ramis, and A. Serra, "From curing kinetics to network structure: A novel approach to the modeling of the network buildup of epoxy–anhydride thermosets," *Journal of Polymer Science Part A: Polymer Chemistry*, vol. 52, no. 1, pp. 61–75, 2014.

[45] A. N. Mauri and C. C. Riccardi, "The effect of epoxy excess on the kinetics of an epoxy–anhydride system," *Journal of applied polymer science*, vol. 85, no. 11, pp. 2342–2349, 2002.

[46] J. Rocks, L. Rintoul, F. Vohwinkel, and G. George, "The kinetics and mechanism of cure of an amino-glycidyl epoxy resin by a co-anhydride as studied by ft-raman spectroscopy," *Polymer*, vol. 45, no. 20, pp. 6799–6811, 2004.

[47] X. Fernández-Francos, A. Rybak, R. Sekula, X. Ramis, and A. Serra, "Modification of epoxy–anhydride thermosets using a hyperbranched poly (ester-amide): I. kinetic study," *Polymer international*, vol. 61, no. 12, pp. 1710–1725, 2012.

[48] K. Dušek, M. Ilavskỳ, and S. Luňák, "Curing of epoxy resins. i. statistics of curing of diepoxides with diamines," in *Journal of polymer science: Polymer Symposia*, Wiley Online Library, vol. 53, 1975, pp. 29–44.

[49] S. Luňák and K. Dušek, "Curing of epoxy resins. ii. curing of bisphenol a diglycidyl ether with diamines," in *Journal of Polymer Science: Polymer Symposia*, Wiley Online Library, vol. 53, 1975, pp. 45–55.

[50] A. M. Tomuta, X. Ramis, F. Ferrando, and A. Serra, "The use of dihydrazides as latent curing agents in diglycidyl ether of bisphenol a coatings," *Progress in organic coatings*, vol. 74, no. 1, pp. 59–66, 2012.

[51] F. Wu, X. Zhou, and X. Yu, "Reaction mechanism, cure behavior and properties of a multifunctional epoxy resin, tgddm, with latent curing agent dicyandiamide," *RSC advances*, vol. 8, no. 15, pp. 8248–8258, 2018.

[52] K. Raetzke, M. Shaikh, F. Faupel, and P.-L. Noeske, "Shelf stability of reactive adhesive formulations: A case study for dicyandiamide-cured epoxy systems," *International journal of adhesion and adhesives*, vol. 30, no. 2, pp. 105–110, 2010.

[53] Y. Lin, H. Sautereau, and J. Pascault, "Processing property relationship for dicyandiamide-cured epoxy networks," *Journal of applied polymer science*, vol. 33, no. 2, pp. 685–691, 1987.

[54] K. Suzuki, N. Matsu-Ura, H. Horii, Y. Sugita, F. Sanda, and T. Endo, "Diethyl ketone-based imine as efficient latent hardener for epoxy resin," *Journal of applied polymer science*, vol. 83, no. 8, pp. 1744–1749, 2002.

[55] K. Suzuki, N. Matsu-ura, H. Horii, Y. Sugita, F. Sanda, and T. Endo, "One-pot curing system of epoxy resin imines initiated with water," *Journal of applied polymer science*, vol. 88, no. 4, pp. 878–882, 2003.

[56] Y. Yang, R. Boom, B. Irion, D.-J. Van Heerden, P. Kuiper, and H. De Wit, "Recycling of composite materials," *Chemical Engineering and Processing: Process Intensification*, vol. 51, pp. 53–68, 2012.

[57] D. García, I. Vegas, and I. Cacho, "Mechanical recycling of gfrp waste as short-fiber reinforcements in microconcrete," *Construction and Building Materials*, vol. 64, pp. 293–300, 2014.

[58] N. Ramawat, N. Sharma, P. Yamba, and M. A. Sanidhi, "Recycling of polymer-matrix composites used in the aerospace industry-a comprehensive review," *Materials Today: Proceedings*, 2023.

[59] P. H. Wang and N. Zimmermann, "Composite recycling techniques: A literature review," *Juniper Online J. Mater. Sci*, vol. 6, no. 1, p. 555 679, 2020.

[60] S. Zhang *et al.*, "Chemical recycling of epoxy thermosets: From sources to wastes," in *Actuators*, MDPI AG, vol. 13, 2024, p. 449.

[61] R. A. Clark and M. P. Shaver, "Depolymerization within a circular plastics system," *Chemical Reviews*, vol. 124, pp. 2617–2650, 2024.

[62] M.-S. Wu, B. C. Jin, X. Li, and S. Nutt, "A recyclable epoxy for composite wind turbine blades," *Advanced Manufacturing: Polymer & Composites Science*, vol. 5, no. 3, pp. 114–127, 2019.

[63] Aditya Birla Chemicals, *Recyclamine: The planet is mine*, 2024. Available: `https://www.adityabirlachemicals.com/pdf/brochure_pdf_url_59_1721802424.pdf`.

[64] Y. Wang *et al.*, "Enhanced mechanical and adhesive properties of pdms coatings via in-situ formation of uniformly dispersed epoxy reinforcing phase," *Progress in Organic Coatings*, vol. 174, p. 107 319, 2023.

[65] Y. C. Kim and J.-R. Lee, "Evidence for the volumetric expansion of n-benzylpyrazinium hexafluoroantimonate and epoxy mixture during curing reaction," *Polymer journal*, vol. 30, no. 11, pp. 925–928, 1998.

[66] G. Socrates, *Infrared and Raman characteristic group frequencies: tables and charts*. John Wiley & Sons, 2004.

[67] J. Clayden, N. Greeves, and S. Warren, *Organic chemistry*. Oxford university press, 2012.

[68] E. V. Anslyn and D. A. Dougherty, *Modern physical organic chemistry*. University science books, 2006.

[69] N. Dorsaz, C. De Michele, F. Piazza, P. De Los Rios, and G. Foffi, "Diffusion-limited reactions in crowded environments," *Physical review letters*, vol. 105, no. 12, p. 120 601, 2010.

[70] J. E. White, H. C. Silvis, M. S. Winkler, T. W. Glass, and D. E. Kirkpatrick, "Poly (hydroxyaminoethers): A new family of epoxy-based thermoplastics," *Advanced Materials*, vol. 12, no. 23, pp. 1791–1800, 2000.

[71] D. L. Pavia, G. M. Lampman, and G. S. Kriz, *Introduction to spectroscopy*. Cengage Learning, 2001.

[72] J. P. Pascault and R. J. J. Williams, *Epoxy polymers : new materials and innovations*. Wiley, 2010.

[73] C. A. May, *Epoxy Resins: Chemistry and Technology*. Wiley, 1988.

[74] F. A. Carey and R. J. Sundberg, *Advanced organic chemistry*. Springer, 2007.

[75] A. Pathania, R. K. Arya, and S. Ahuja, "Crosslinked polymeric coatings: Preparation, characterization, and diffusion studies," *Progress in Organic Coatings*, vol. 105, pp. 149–162, 2017.

[76] A. Shrivastava, *Introduction to plastics engineering*. William Andrew, 2018.

[77] A. Kinloch, "The science of adhesion: Part 1 surface and interfacial aspects," *Journal of materials science*, vol. 15, pp. 2141–2166, 1980.

[78] V. Basin, "Advances in understanding the adhesion between solid substrates and organic coatings," *Progress in organic coatings*, vol. 12, no. 3, pp. 213–250, 1984.

[79] F. Awaja, M. Gilbert, G. Kelly, B. Fox, and P. J. Pigram, "Adhesion of polymers," *Progress in polymer science*, vol. 34, no. 9, pp. 948–968, 2009.

[80] S. Lipatov, *Polymer reinforcement*. ChemTec Publishing, 1995.

[81] E. M. Petrie, *Epoxy Adhesive Formulations*. New York: McGraw-Hill, 2006.

[82] Y. Miao, W. Du, J. Yin, Y. Zeng, and C. Wang, "Characterizing multi mechanical behaviors for epoxy-like materials under wide strain rate range," *Polymer Testing*, 2022.

[83] S. Ebnesajjad, *Handbook of Polymer Applications in Medicine and Medical Devices: 6. Adhesives for Medical and Dental Applications*. Elsevier Inc. Chapters, 2013.

[84] P. I. Abronina, N. N. Malysheva, A. I. Zinin, N. G. Kolotyrkina, E. V. Stepanova, and L. O. Kononov, "Catalyst-free regioselective acetylation of primary hydroxy groups in partially protected and unprotected thioglycosides with acetic acid," *RSC advances*, vol. 10, no. 60, pp. 36 836–36 842, 2020.

[85] R. J. Young and P. A. Lovell, *Introduction to polymers*. CRC press, 2011.

[86] R. A. O. Bernal, R. O. Olekhnovich, and M. V. Uspenskaya, "Influence of thermal treatment and acetic acid concentration on the electroactive properties of chitosan/pva-based micro- and nanofibers," *Polymers*, vol. 15, no. 18, p. 3719, 2023.

[87] P. Gahtori, V. Gunwant, and R. Pandey, "Role of hydrophobic side chain in urea induced protein denaturation at interface," *Chemical Physics Impact*, vol. 7, p. 100 314, 2023.

[88] V. Simril, "Internal plasticization: The effect of chemical structure," *Journal of Polymer Science*, vol. 2, no. 2, pp. 142–156, 1947.

Appendix A: Pre-analysis 7

This appendix documents the preliminary experimental attempts aimed at understanding the behavior of the material. While detailed analyses of the second and third batches are presented in the main body of the thesis, this section highlights earlier trials, including those that did not yield meaningful results. In cases where experimental inconsistencies or failures were evident, further in-depth analyses were not pursued, as the data were clearly unsuitable for reliable interpretation. Some further trials have even not been documented as not relevant.

A.1 First Batch

A.1.1 Recycling and Precipitation

The recycled solution of acetic acid and dissolved laminate matrix was poured into a 5 wt% aqueous solution of sodium hydroxide. The obtained polymer had a yellowish colour with the consistence of honey.

A.1.2 Sample denomination

The recycled polymer non-thermally treated is denominated RP0, the recycled polymer dried in vacuum oven over night at 60 °C is RP60, the recycled polymer dried in vacuum oven for 30 min at 100 °C is RP100-1, RP100-1 dried further in vacuum oven for 15 min at 100 °C is RP100-2, and the RP100-2 sample heated further 10 min at 100 °C is RP100-3.

A.1.3 FTIR

The recycling of the polymer by using a 30% acetic acid aqueous solution was shown to a be partially selective degradation. Indeed, the FTIR results (Figure 7.1a) show a selective cleavage of C−O ketal bond, leaving the alky-aryl C−O and C−C bond of the skeleton structure intact. The absorbance peaks at 1209, 1155 and 1078 cm^{-1} (Figure 7.1b) corresponding to the C−O−C−O−C stretching vibration of the ketal linkage, present in the hardener and in the cured epoxy graphs disappear in the recycled polymer samples, which indicates the cleavage of the C−O bond during the recycling process. C−N bonds with the formation of secondary amines. The presence of hydrogen-bonding of the types O−H $\cdots$ O creates intermolecular interactions, as demonstrated by the broad peak at 3380 cm^{-1}. The increase in intensity of the hydroxyl group stretching vibration band supports the formation of -OH end groups from the hydrolysis of ketal linkages. The presence of tertiary amines was not possible to detect.

With regard to the skeleton structure, the peak at 1239 and 1035 cm^{-1} belonging to the asymmetrical and symmetrical aryl-alkyl ethers =C−O−C- stretching vibration, respectively, appears in the spectra of recycled polymer samples, indicating the preservation of the aryl-alkyl ether bonds. The peaks of the C=C stretching vibration of the benzene ring appear at 1607, 1582,

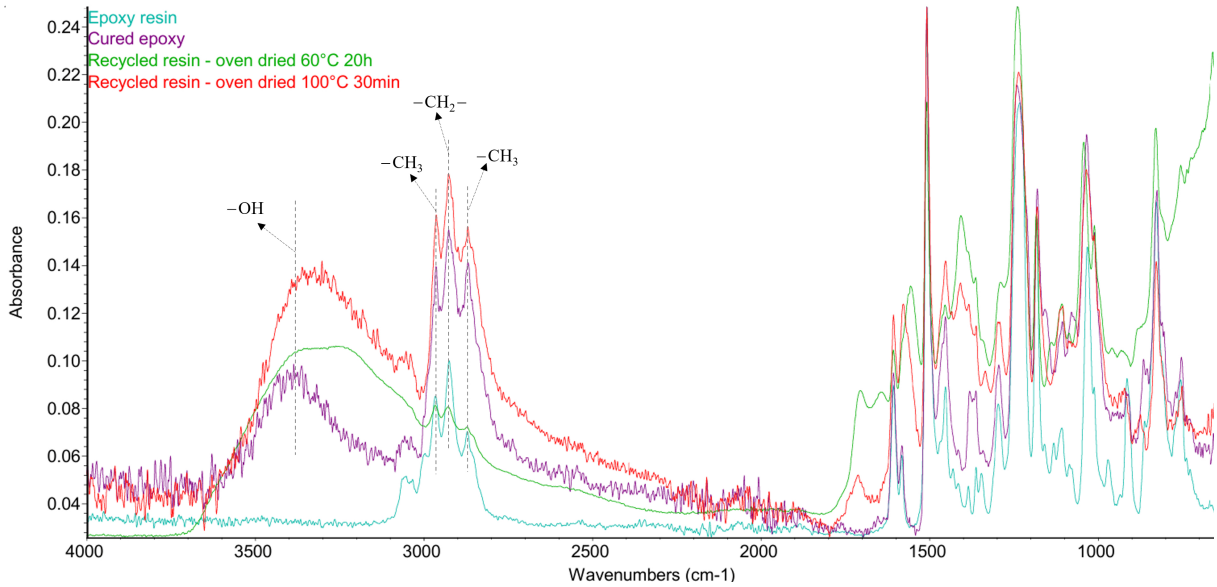

(a)

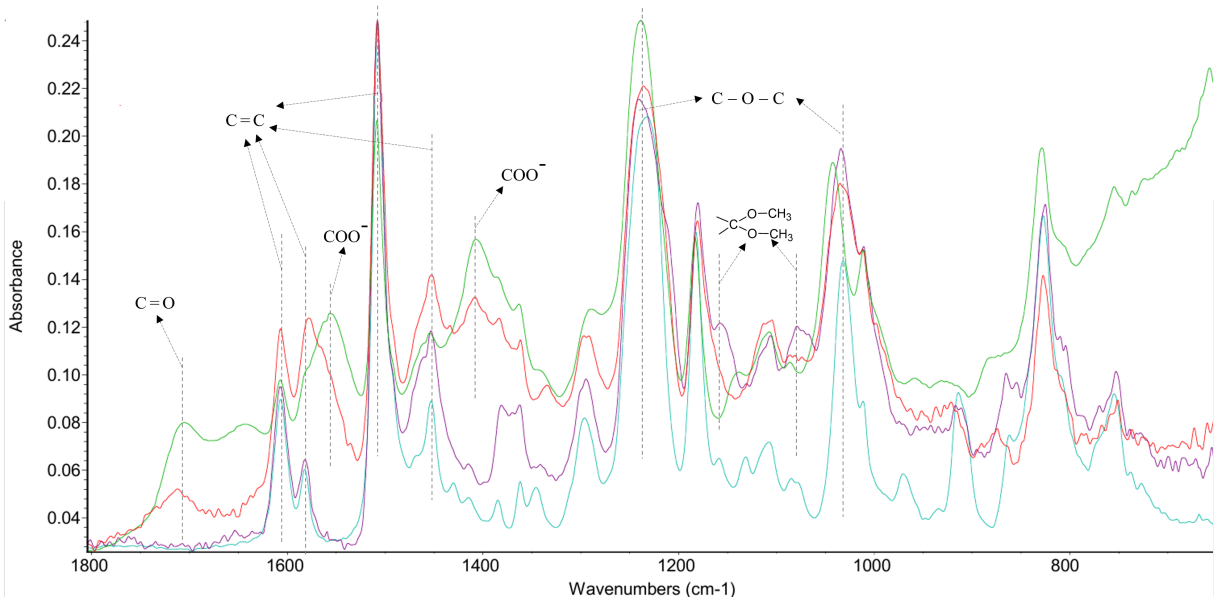

(b)

Figure 7.1: FTIR spectra of (a) the epoxy resin (blue), the cured epoxy (purple), the recycled polymer dried in vacuum oven over night at 60 °C (green) and for 30 min at 100 °C (red); (b) enlargement of the fingerprint region of the spectra in (a).

1507 and 1454 cm^{-1} and are also present in the recycled polymers, suggesting that the structure of the aromatic rings remains intact. The peak at 1705 cm^{-1}, found in the recycled products, belongs to the C=O stretching vibration of acetic acid remained in the polymer. Indeed, the mild nature of acetic acid inhibit the possible formation of ester bond by esterification reaction with the C−OH of the cured epoxy unit. The quantity of water present in the samples is shown clearly from the peak at 1643 cm^{-1}, associated with the H−O−H deformation vibration. The significant decrease from RP60 sample to RP100-1, shows that a higher temperature treatment is necessary to dry the produced recycled polymer fully. In the spectrum of RP60, the signals at 1555 and 1407 cm^{-1} correspond to the antisymmetric and symmetric stretching vibration, respectively, of carboxylate ion COO^-, which indicate the acetic acid is deprotonated during the neutralization process. The presence of acetic acid in the polymeric structure can be explained by the formation of strong interaction, such as hydrogen-bonging, between the AcCOOH molecules and polar functional groups in the polymer chains. A further hypothesis was the partial acetylation of primary hydroxy groups [84]. However, this consideration was discarded due to the absence of characteristic absorbance peak of ester bond (product of the esterification with acetic acid). The characteristic peak relative to the stretching vibration absorption of the epoxy group can be seen only in the epoxy resin at 913 cm^{-1}.

Table 7.1: FTIR

Wavenumber (cm^{-1})	**Vibration type**	**Assignment**
3380	O-$H_{H-bond(itermolecular)}$ stretching	—OH
2965	*asym.* C-H stretching	$—CH_3$
2923	C-H stretching	$—CH_2—$
2871	*sym.* C-H stretching	$—CH_3$
1705	C=O stretching	—COOH (acetic acid)
1643	H-O-H scissor bending	H_2O
1607	C=C stretching	Aromatic ring
1582		
1555	*asym.* COO^- stretching	COO^- carboxylate ion (acetic acid)
1507	C=C stretching	Aromatic ring
1454		
1452	-CH_2 deformation	$—OCH_2—$
1407	*sym.* COO^- stretching	COO^- carboxylate ion (acetic acid)
1382	-CH_2 wagging	$—OCH_2—$
1361	C-H deformation	$—C(CH_3)_2—$
1294	C-C twisting	$—CH_2—$
1239	*asym.* C-O-C stretching	═COC—
1209	C-O stretching	C−O−C−O−C
1181	C-O stretching	—OH
1155	C-O stretching	C−O−C−O−C
1109	C-O stretching	—OH
1078	C-O stretching	C−O−C−O−C
1035	*sym.* C-O-C stretching	═COC—
913	C-O stretching	Epoxy group
862, 828.1	*out-of-plane* C-H deformation	Aromatic ring

A.1.4 DSC

The gradual decrease in the glass transition temperature from 81.21 °C of the RP0 sample to 64.50 °C of the RP100-3 sample is evinced in Figure 7.2, and the T_g of each sample is reported in Figure 7.3. Changes in glass transition temperature can be provoked by several factors, such as changes in molar mass, amount of branching and crosslinking, changes in free volume, and intermolecular forces [85]. According to the results collected, the decreasing trend shown by the T_g might be due to the evaporation of water, observed also in the FTIR with the disappearance of the peak at 1643 cm^{-1}. Indeed, the evaporation could reduce the amount of hydrogen-bounding, hence increasing the free volume. An increase in free volume would comport a greater mobility of the polymer chains at lower temperature, therefore less thermal energy is required to free the backbone, which comports a lower T_g. On the other hand the possible degradation of the chains would comport a decrease in molar mass and an increase in free volume, also lowering the T_g.

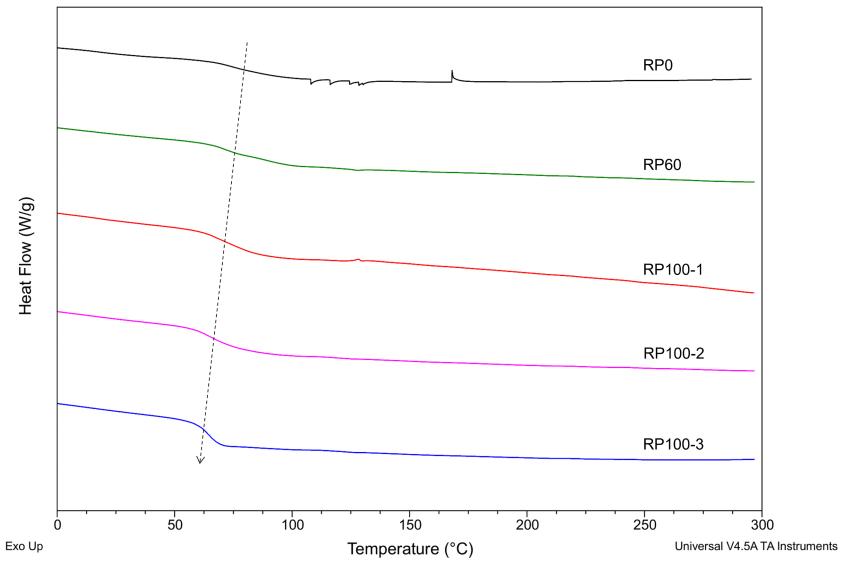

Figure 7.2: DSC thermograms of the studied samples with highlight to the glass transition temperature from the second heating cycle.

Some amorphous polymers may undergo molecular reorientation, especially if they have polar side groups. This reorganization can lead to reduced intermolecular forces, resulting in lower T_g.

Moreover, the absence of a melting peak signify that the polymer is completely amorphous. Indeed, amorphous polymers do not present a melting temperature (T_m) but only a glass transition temperature.

A.1.5 TGA

Thermogravimetric analysis (TGA) of the recycled polymer samples show that except for sample RP100-2, the weight loss (%) of the recycled polymers happened in two stages. The derivative thermogravimetric (DTG) curves shows that the first weight loss happens in between 50-240 °C, associated with the evaporation of moisture and residual solvent. Indeed, acetic acid has a boiling point of 118°C, but if part of the polymeric structure due to strong interactions (e.g. hydrogen bonding), it might not just boiling off, like a pure liquid, but slowly desorbing or diffusing out of the polymer structure increasing the temperature of boiling [86]. A decrease in weight loss of

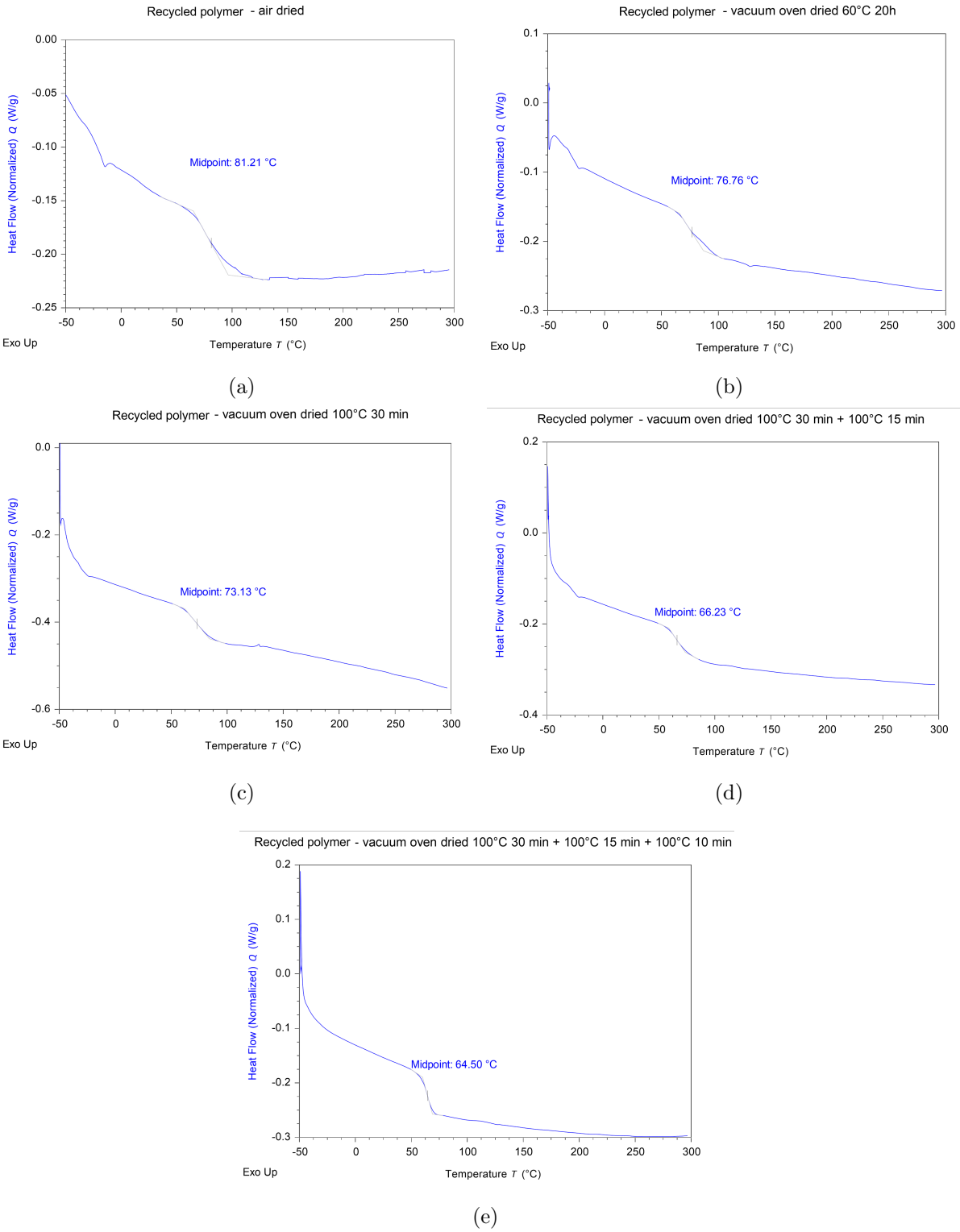

Figure 7.3: DSC thermograms showing the glass transition temperature (T_g) from the second heating cycle of (a) RP0, (b) RP60, (c) RP100-1, (d) RP100-2, (e) RP100-3.

the first stage with the increase of drying was observed (Figure 7.4). The non-thermally treated recycled polymer showed a 34.165% weight loss, against the 29.113% of the RP60 sample and 12.979% of RP100 sample. This support the correlation of the first peak in the DTG curves with the moisture and solvent desorption. The second step is related to the polymer chains thermal destruction.

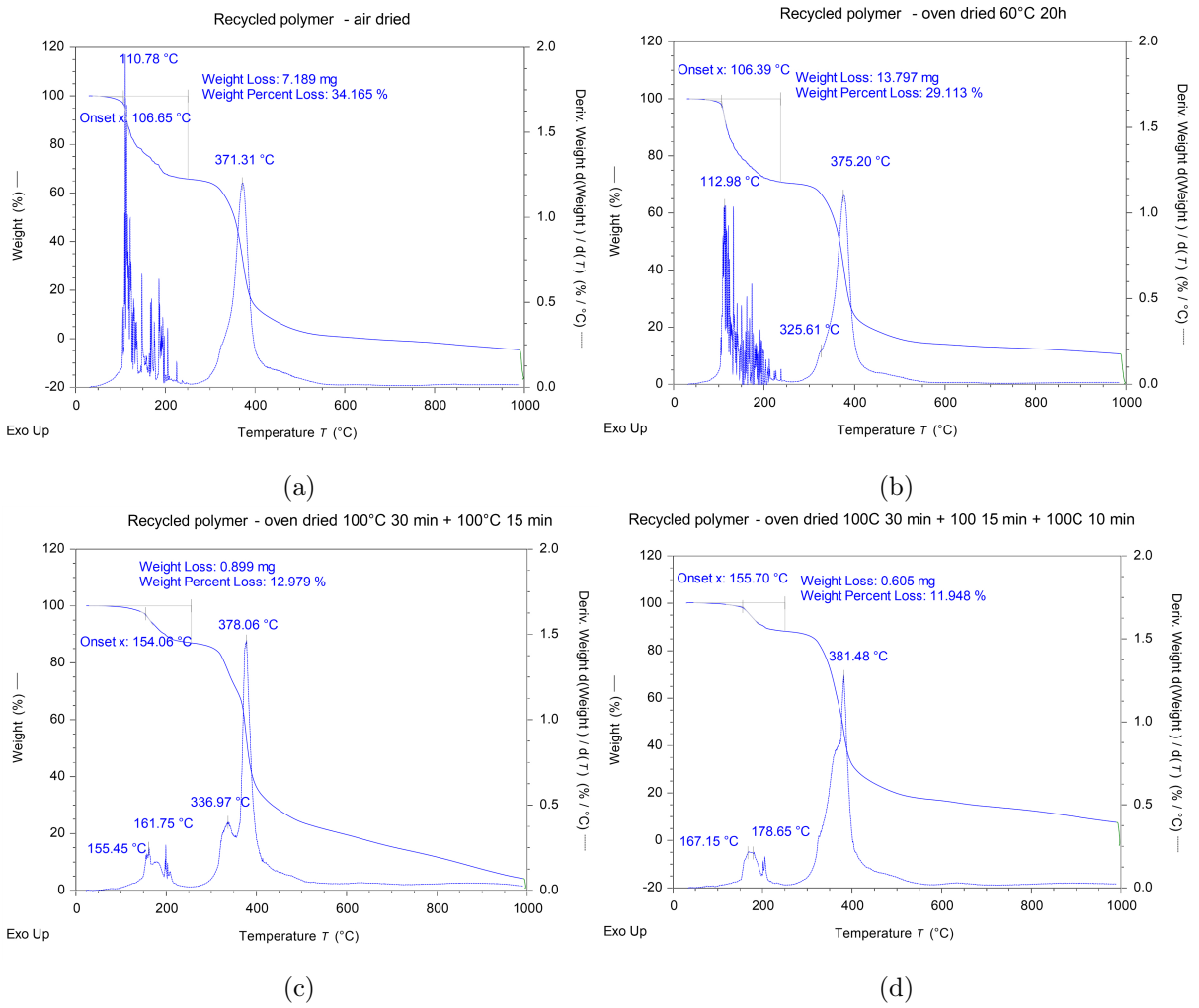

Figure 7.4: TGA thermograms showing the (a) RP0, (b) RP60, (c) RP100-1, (d) RP100-2, (e) RP100-3.

A.1.6 Hydrogen bonding analysis

In order to define the nature of the crosslinking present in the recycled polymer a simple analysis using an 8 M aqueous urea solution was performed. A sample of RP100 was immersed in the urea solution and left it in for 24 hours. After one day the recycled polymer sample was totally dissolved in the solution, suggesting a high concentration of hydrogen bonds forming physically cross-linked networks. Indeed, sure is known for its ability to break hydrogen bonds [87].

A.2 Second Batch

A.2.1 Recycling and Precipitation

The recycled solution of acetic acid and dissolved laminate matrix was poured, in this case, into a 10% wt aqueous solution of sodium hydroxide. The obtained polymer was then washed three times in fresh NaOH solutions, in order to neutralize the acid. Successively, the obtained polymer was washed in deionized (DI) water (Figure 7.5a. This step was necessary to remove sodium acetate ($CH_3COO^-Na^+$) from the solution, thanks to its deliquescent and hygroscopic nature. Nonetheless, the pH of the obtained polymer was very alkaline, as reported in Figure 7.6, probably due to the high concentration of NaOH taped in the polymer molecules. Therefore, several washes with DI water were performed until a stable pH was reached. The final polymer appeared as a

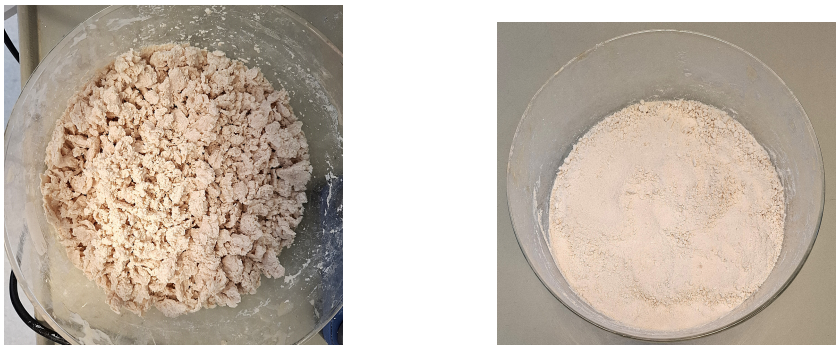

(a) (b)

Figure 7.5: (a) recycled polymer washed 3 times in NaOH 10 wt% solution and then rinsed with DI water; (b) recycled polymer washed 3 times in NaOH 10 wt% solution and then rinsed 8 times with DI water, then air dried.

powder (Figure 7.5b) with a pH of 5. The acidic pH of the obtained polymer could be due to the presence of acetic acid in the structure of the polymer, by hydrogen bonding interactions. Indeed, the FTIR spectrum, reported in Figure 7.7, shows that, even though almost totally disappeared, the peak associated with the carbonyl group in the acetic acid molecules is still present (see 7).

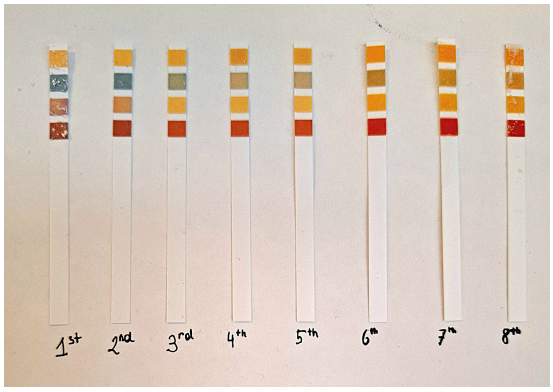

Figure 7.6: Variation of pH during the different washes of the recycled polymer obtained in the second batch.

To evaluate the weight percentage of water in the powder, a simple measurement was performed. 1 g of powder was weighed and placed in the oven at 40 °C overnight. The results showed that no change in weight was present, defining that the material was totally dried.

A.2.2 FTIR

In Figure 7.7 the spectra of the cured epoxy, RP0, the RP obtained in the second batch before and after drying are reported.

The peak at 1705 cm^{-1} relative to the stretching vibration of C=O acetic acid molecules present in the polymer has disappeared almost completely in the RP washes multiple times in NaOH and DI water. Moreover, the signals at 1555 and 1407 cm^{-1} correspond to the antisymmetric and symmetric stretching vibration, respectively, of carboxylate ion COO^- are also not present in the turquoise and red spectra. This indicates that the washing process was successively able to remove the presence of acetic acid from the polymer structure.

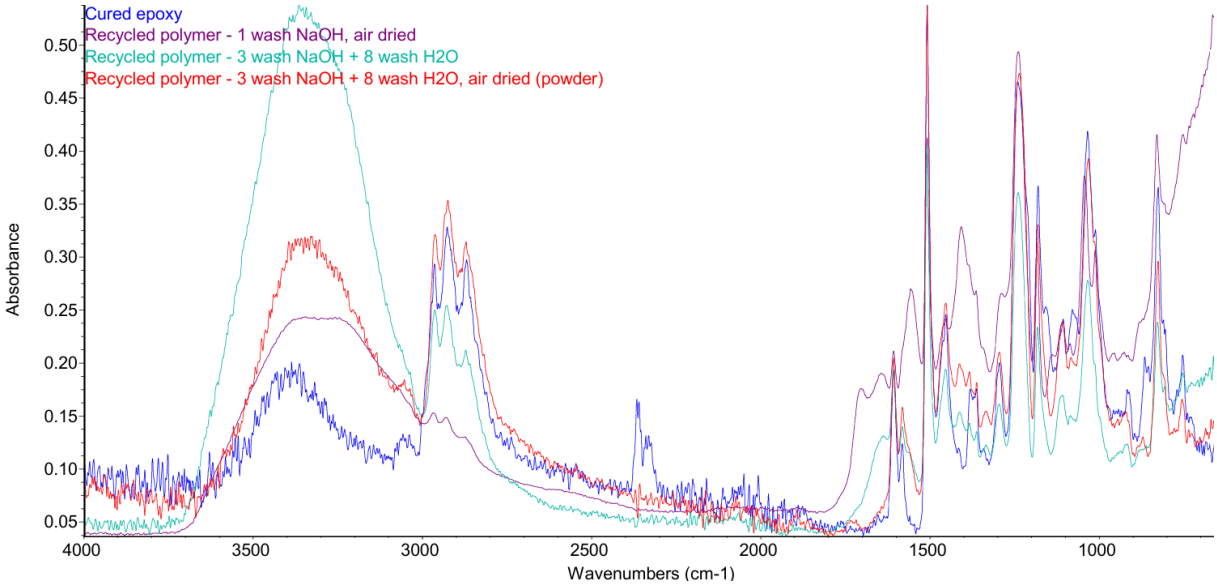

Figure 7.7: FTIR spectra of the cured epoxy (blue), RP0 from first batch (purple), RP 3 times washed in 10% wt NaOH solution and then washed 8 times in DI water (turquoise) and RP 3 times washed in 10% wt NaOH solution and then washed 8 times in DI water after drying (red).

A.2.3 DSC

In Figure 7.8 the DSC thermogram of the recycled polymer powder reporting the glass transition temperature from the second heating cycle.

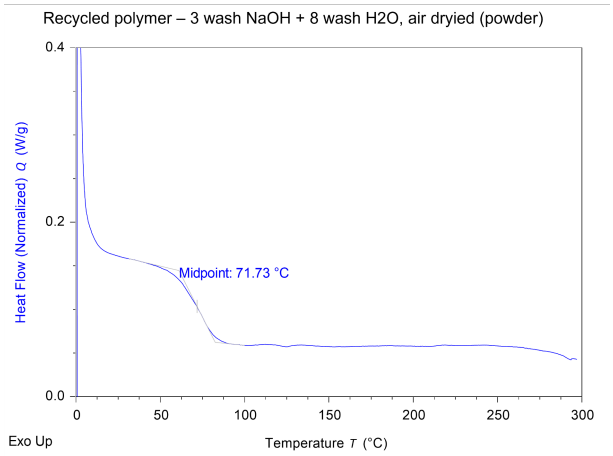

Figure 7.8: DSC thermograms showing the glass transition temperature (T_g) from the second heating cycle of the recycled polymer powder obtained after 3 washes in 10% wt NaOH solution and successively washed 8 times with DI water

The glass transition temperature is the temperature below which a polymer turns from a hard and brittle material to a ductile material. Below T_g there is no rotation about the polymer backbone. The atoms of the polymer chains are fixed in a given geometric spatial configuration, where no large-scale polymer chain motion is present. This little mobility of the polymer chains is a result of the change in physical properties to the ones of a rigid, glassy state. Above T_g the carbon chains start to moving, comporting a transition to a flexible, rubbery state. When the ambient temperature is below T_g, the polymer chains are fixed in place and behave like a solid glass. As above mentioned signify that the recycled polymer, which T_g is 71.73 °C, at room temperature has a brittle, glassy material.

A.3 Third Batch

In this case, the recycled polymer obtained by neutralizing the recycled solution of acetic acid and dissolved laminate matrix in a 10 wt% aqueous solution of sodium hydroxide was washed only once in NaOH solutions.

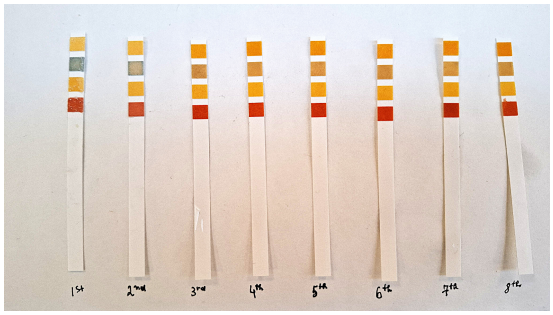

Figure 7.9: Variation of the pH along the washing of the recycled polymer obtained in the third batch.

Whereas, the other steps were left the same. In this case the pH was also monitored, but presented different results, as displayed in Figure 7.9. Indeed, the pH of the first wash is about 7 and it stabilizes at 5 already at the third wash.

The RP powder was used, also in this batch, to prepare an RP solution in 30% wt AcCOOH. The steps to arrive to a 95% w/v RP solution are reported in Figure 7.10.

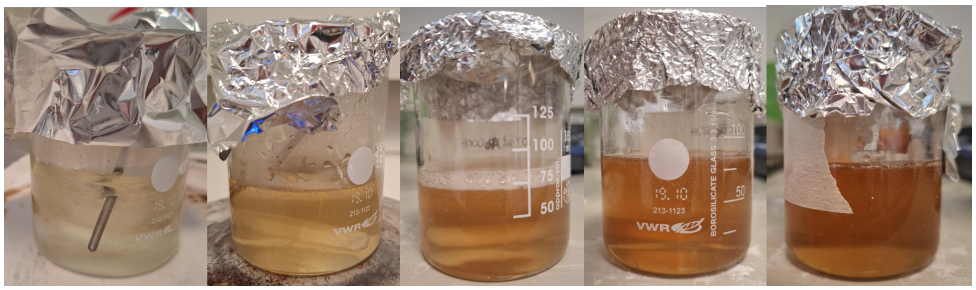

Figure 7.10: Different steps of the RP in 30% wt acetic acid solution preparation. From left to right a) 15% w/v, b) 30% w/v, c) 50% w/v, d) 90% w/v and e) 95% w/v.

A.3.1 FTIR

Figure 7.11 compares the FTIR spectrum of the RP powders produced in the second and third batch.

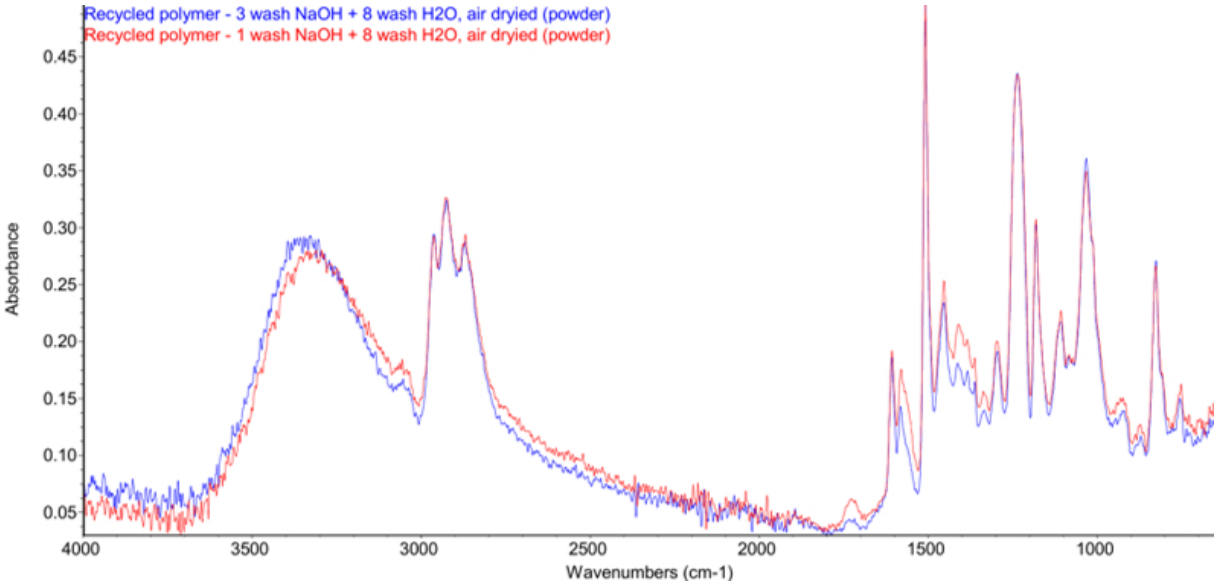

Figure 7.11: FTIR spectra of RP powder 3 times washed in 10% wt NaOH solution and then washed 8 times in DI water, air dried (blue) and RP powder washed once in 10% wt NaOH solution and then washed 8 times in DI water after drying (red).

A.3.2 DSC

The RP powder produced in this last batch presented a small decrease in T_g as illustrated in Figure 7.12. This trend might be associated with a higher concentration of AcCOOH molecules, as abovestated. Indeed, the introduction of a foreign molecule into the polymer chain will alter the local mobility of chains and the magnitude of inter- and intramolecular forces, by acting as an internal plasticizer [88]. This disruption of the regular packing and organization of the chain, increases the free volume and enhances the inner mobility, reducing the thermal energy required for molecular motion, thereby lowering the T_g.

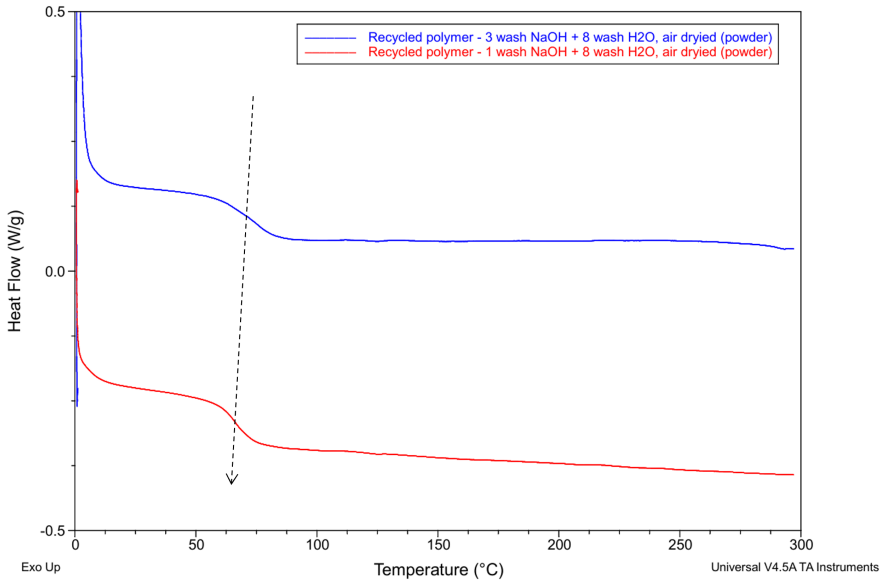

Figure 7.12: Comparison of the DSC thermograms of the RP powder from the second batch (blue) and the third batch (red), with highlight to the glass transition temperature from the second heating cycle.

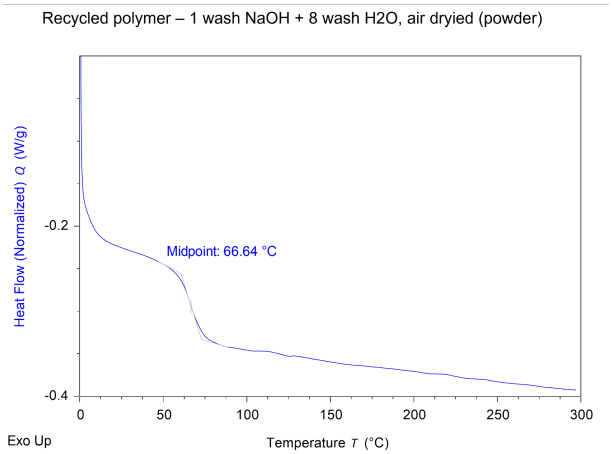

Figure 7.13: DSC thermograms showing the glass transition temperature from the second heating cycle of the recycled polymer powder obtained, after 1 wash in 10% wt NaOH solution and successively washed 8 times with DI water.